Attachment D1
Capital Improvement Plans and Other Significant Port Developments Anticipated During the Period of the Proposed Action

Port	*Improvements and Other Significant Developments*
Baltimore, MD	The Board of Public Works approved the purchase of a new $7.4 million container crane to be installed at the Dundalk Marine Terminal, a 231 ha (570 acre) terminal complex with 13 deepwater berths and 9 container cranes. The new crane is expected to be operational by early 1995 (Governors Press Office, State of Maryland, May 18, 1994). Governor William Schaefer announced Board of Public Works approval of a contract to modernize and improve (up-grade to post-Panamax capacity) three container cranes located at the Dundalk Marine Terminal (Ibid, June 22, 1994).
Boston, MA	Officials of the Massachusetts Port Authority (Massport) have submitted a draft environmental impact report to Federal and State officials that calls for dredging the harbor and access channels to 12.2 m (40 ft) from 9.75-10.97 m (32-36 ft) (*American Shipper*, "Boston Seeks Direct Calls From Asia," October 1994, Pg. 94). Ralph Cox, Marine Director, and other port officials claim that the deeper water is critical to the Port's viability. Massport is also seeking support of the State Legislature for road and rail clearances to permit double-stack train service to the City of Boston and its marine terminals. A $50 million expansion and modernization of Boston's Conley Terminal is approximately 80 percent complete. When completed, Conley Terminal will have 40.5 ha (100 acres) of container storage and handling area, 4 post-Panamax container cranes, 304.8 m (1,000 ft) of berth, and a new gate complex. Reportedly, container tonnage is up for 1994 over 1993 tonnage when Boston handled 152,240 twenty-foot equivalent units for the year.
Charleston, SC	As of late 1993, the $90 million Wando terminal expansion project was nearing completion. When completed, the project will add an additional 418.5 m (1,373 ft) of berthing space, 26.3 ha (65 acres) of container storage area, and two $5.4 million post-Panamax container cranes. The entire project is scheduled for completion by Fall 1994. Planning is progressing for development of the approximately 323.8 ha (800-plus acre) Daniel Island terminal site in Charleston Harbor. The container terminal is being designed to meet demand at the port well into the 21st century. The massive project is expected to take 15 to 20 years to complete and will ultimately consist of 323.8 ha (800 acres) of paved container storage and 2,438 m (8,000 lineal ft) of berthing space (*American Shipper* - Southern Ports, January 1994). At NWS Charleston, the U.S. Army is planning to expand Wharf Alpha and upgrade the railroad in support of the Army Strategic Mobility Logistics Base. This upgrade is scheduled for completion in 1998.

Concord NWS, CA	Currently authorized improvements expected to be completed by 1997 include an upgrade of Pier 3 to withstand greater loadings, and will also include two new 36 metric ton (40 ton) container cranes, container storage pads, and support facilities and equipment. These improvements are projected to permit average load rates of about 20 containers per hour. The improvements will also permit increasing the channel depth and depth alongside to 12.7 m (42 ft) in the future if necessary. The facility will be the designated West Coast container facility for military shipments (personal communications from Karl Yocum, Concord NWS Office of Business Development, September 1, 1994, and 1994 Fact Sheets received during port visit).
Eddystone, PA	No immediate improvements identified.
Fernandina Beach, FL	U.S. Army Corps of Engineers is expected to award a contract in October 1994 for deepening of the harbor channel to 11 m (36 ft), and to construct a 366 m (1,200 ft) turning basin (Personal communication from Mr. Stubbs, Port of Fernandina, September, 1994).
Gulfport, MS	A consulting firm has recommended a 15-year, $160 million terminal expansion for the Port of Gulfport to a projected tripling of port business by 2010. The proposed expansion would add 34 ha (84 acres) of land to West Pier at a cost of $81 million, replace or reconfigure existing warehouses ($13 million), and include the purchase of $11 million in additional container handling equipment (but not necessarily a container gantry crane) (*American Shipper*, September 1994, p. 102; *Containerization International*, September 1994, p. 11). A $41 million dredging project that deepened the harbor from 9.14 m to 10.97 m (30-36 ft) was completed in April 1994. In August 1993, the Port Authority issued $15 million in bonds to pay for three development projects that included expansion of East Pier warehouse facilities and the addition of 11.7 ha (29 acres) of land—through diking and pumping sand, at West Pier. The latter to be used for a new container terminal (*American Shipper* - Southern Ports, January 1994).
Jacksonville, FL	In anticipation of continued strong growth in cargo demand over the next 20 years, JAXPORT adopted a 20-year, $934 million development plan designed to prepare its facilities for 2010. In addition to recommendations for immediate construction of a third container terminal at Dames Point, consultants recommended expansion and reconfiguration of the Authority's Blount Island and Talleyrand Terminals, projected to cost about $274 million over 7 years. A $1 million feasibility cost sharing agreement was signed this year with the Corps of Engineers to develop a dredging study to deepen the harbor from 11.6 m (38 ft) to 12.8 m (42 ft). Design of a second roll-on/roll-off dock plus 2 ha (5 acres) more container storage and a 450 m (1,500 ft) extension of marginal wharf is scheduled for Blount Island in fiscal 1995 [The Jacksonville Port Authority (JAXPORT), Marketing Department, October 3, 1994].

The Port Authority anticipated breaking ground in 1994 for a new 203 ha (500 acre) container and general cargo terminal complex at Dames Point, immediately adjacent and upstream of its existing Blount Island terminal. The new facility is expected to cost $160 million when completed in the future. Other improvements scheduled include a $2.5 million investment in increased intermodal rail capacity at Blount Island and Talleyrand Terminals, and widening of Hecksher Drive to four lanes from the entrance to Blount Island to State Road 9A, which connects with I-95. I-295 is also being widened to four lanes (American Shipper - Southern Ports, January 1994).

Long Beach, CA

The Long Beach Port Commission and City Council have approved a 1994-95 budget of $417 million, which includes $236.5 million for port construction, land acquisition, and environmental mitigation. Last year's budget included $405 million to purchase land owned by Union Pacific Resources Company in the north harbor, which the Port plans to convert to a marine cargo terminal. The property is comprised of 117 ha (289 acres) north of the Cerritos Channel, 143 ha (354 acres) south of the Channel, and 33 ha (82 acres) within the Channel. The new budget provides allocations of $60 million for street overpasses to cross rail lines in the port area, $22 million for other street and road improvements, $78 million for continuing container terminal improvements at Pier J, $25 million for other construction projects, and $40 million for land acquisitions and environmental mitigation. These land acquisitions will increase the Port's operating area by 35 percent (American Shipper, September 1994, p. 94; "Long Beach to Spend $417 million").

Los Angeles, CA

Los Angeles' "2020 Program" represents the Port's comprehensive long-term development plan, which is designed to accommodate a doubling of cargo throughput through the next decade and a forecast California population of 20 million people. The major components of the 2020 Program include:

a. Construction of Pier 300 on landfill completed in 1983. When completed, Pier 300 will include the American President Lines container terminal, an intermodal container/rail/truck transfer facility and a coal export terminal;

b. Landfill and construction of Pier 400, with three container terminals, an intermodal container transfer facility, and liquid bulk terminals;

c. The Alameda Corridor, a road and rail improvement program linking the Port to rail facilities in downtown Los Angeles with a fully grade-separated trackage (Port of Los Angeles, Property Management Division, October 3, 1994).

Implementation of the 2020 Program is well underway and will involve expenditures of approximately $600 million over the next three years. Work has begun on the new 91.5 ha (226 acres) American President Lines Container Terminal on Pier 300 which, when completed in 1997, will be the largest container terminal in the United States. Costing about $270 million, the terminal will have 1,219 m (4,000 ft) of wharf capable of handling four of American President Lines' largest ships at one time, and an adjacent 19 ha

(47 acre) intermodal rail yard that will also serve the coal export yard being constructed next to the facility. The American President Lines complex will be equipped with six to eight new-generation container cranes. The Port has also embarked on a mammoth $148.6 million dredging project that will create 4.8 km (3 mi) of new channels 13.6 m to 19.1 m (45-63 ft) deep, providing access to Pier 300, a turning basin, and 1,520 m (5,000 ft) of berthing space south of Pier 300. Dredge spoil will be used to create about 91 ha (225 acres) of new land to be called Pier 400, which will be located south (seaward) of the new American President Lines Terminal. Plans for Pier 400, call for the construction of three container terminals on the north side of the terminal, each with two berths and five container gantry cranes, and a large bulk liquid/petroleum terminal complex on the south (ocean) side. Other on-going improvement projects include replacement of the Badger Avenue Bridge providing rail and road access to Pier 300 and Terminal Island, construction of a $200 million coal export terminal on Pier 300 and a $20 million rail yard to serve Terminal Island container terminals [*Long Beach Press Telegram* (Business), "Port Builds for Future," September 26, 1994].

Miami, FL

Phase I of Miami's $100 million port deepening project (begun in April 1991), was completed July 1993 and included deepening of the harbor channel to 12.8 m (42 ft) from the sea buoy to the Lummus Island Container Terminal. Phase II (now underway) extends the 12.8 m (42 ft) channel from container berths on Lummus Island to a new south channel turning basin between Dodge and Lummus Islands. Completion of dredging is expected by mid-1995. The dredging project has already added 24.3 ha (60 acres) of land to Lummus Island and current dredging is expected to add another 16.2 ha (40 acres) for additional container and roll-on/roll-off ship berths. The Port also plans to add two 49 metric ton (54 ton) post-Panamax size container cranes to the existing three 49 mt and three 39.2 metric ton (43 ton) gantry cranes already installed (American Shipper-Southern Ports, January 1994).

Mobile, AL

The Port has just completed about $80 million in improvements through 1993. No new immediate improvements have been identified (Alabama State Docks System, "Port of Mobile Handbook," 1993).

New Orleans, LA

The newest terminal to be added to the Port of New Orleans is the Nashville "B" multi-purpose facility, which marked the completion of the first phase in the ongoing $200 million capital improvements program which, as part of the Mississippi River Terminal Complex, will take New Orleans into the 21st century. When complete, it will feature two miles of continuous modern wharves and state-of-the-art facilities. A full array of multipurpose and ocean-going container ships will be able to discharge cargo quickly, take on new cargo and sail for the next port without delay. A newly paved marshalling yard will eliminate trucking congestion and tie-ups, and an increased shedded area will allow stevedores to operate more efficiently. Flood protection barriers are being raised to eliminate the possibility of flooding. Two ship berths have been added and three more are scheduled to open by the end of 1995. The Napoleon Avenue Wharf C apron width will be replaced to increase the load capacity to 36 kg sm (850 psf), along with other

	improvements. The Tchoupitoulas Corridor Project will provide a new, high-speed dedicated roadway from the port through the city (Annual Directory, Port of New Orleans, 1993-1994; Board of Commissioners of the Port of New Orleans, "Mississippi River Terminal Complex," 1993).
Newport News, VA	No immediate improvements identified.
Norfolk, VA	In 1991, the Virginia Ports Authority began a $40 million expansion of the Norfolk International Terminal that will double the size and cargo handling capacity of the terminal. When completed in 2004, improvements include adding 1,300 m (4,300 ft) of new berthing space and 120 ha (300 acres) of backup cargo handling area, creating a massive (819 acre) intermodal terminal with 27,000 m (89,000 ft) of onsite rail, connecting the terminal with Norfolk Southern's bullet train and providing double stack service to major U.S. markets (Virginia Port Authority, "Promises, Results," 1993; Financial World, "The Ports of Virginia: Destiny Controlled," p. 63, New York, NY, July 20, 1993).
Oakland, CA	The $50 million reconstruction of Oakland's 22.7 ha (56 acre) Seventh Street Terminal is nearing completion. Severely damaged in the 1989 Loma Prieta earthquake, three new post-Panamax cranes have been added and the entire wharf structure and upland areas have been rebuilt. The final phase of the redevelopment program is a $5 million gate relocation and construction project providing six entry and four exit lanes. Truck queues outside the terminal will be avoided by the addition of 46 inbound and 44 outbound queue spaces plus six "trouble" lanes for trucker paperwork problems within the gate area. The gate complex will use computer and video technology to speed container movements through the Port (American Shipper, August 1994, "Rebirth for Oakland Terminal," p. 77).
Philadelphia, PA	A new bi-state agency, *The Port of Philadelphia and Camden, Inc.*, has been created to assume responsibility for regional port operations previously directed by the Philadelphia Regional Port Authority (ports of Philadelphia), the South Jersey Port Corporation (terminals in Camden), and the World Trade Division of the Delaware River Port Authority—a regional economic development agency. The new agency will begin operation in 1995 (WWS/World Wide Shipping, June 1994, p. 35).
Port Everglades, FL	Completion of the Port Everglades Authority's new $100 million, 62.7 ha (155-acre) container complex at Southport, and the development of 6.7 ha (15 acres) of expanded container storage area at Midport, both scheduled for 1994, culminates years of planning and construction by Port Everglades. Southport is equipped with three 39.2 metric ton (43 ton) low-profile, post-Panamax container cranes designed to avoid interference with nearby airport operations. Design planning studies are underway for lift-on/lift-off support facilities at the new 26 ha (63 acre) lift-on/lift-off container yard located immediately adjacent to Southport's cranes. These include a container freight station, electrical outlets for reefer containers, gatehouse with scales, inspection shed, automated facilities, and a feasibility study for developing an intermodal container transfer facility nearer to the Southport complex. The

Fiscal 1993-94 budget provides $9.6 million for a tenth cruise line terminal and enhancements to the two facilities described above (FS, 1992; Southern Ports, January 1994, Pg. 33).

Port of New York, NY

The Port Authority of New York/New Jersey's 1993 capital spending budget totaled $57 million, largely for terminal improvements such as wharf rehabilitation, berth deepening, paving, etc.

Port of Elizabeth, NJ

Funds were also included for deepening Federal channels in the Kill Van Kull and into Newark Bay to the Elizabeth Marine Terminal. The total project, scheduled for completion in 1995, will provide a 12.2 m (40 ft) channel from Upper New York Bay through the Kill Van Kull into Newark Bay. The lack of adequate channel depths has resulted in the diversion of ships to other ports. Three and a half years of wrangling over permits for maintenance dredging and ocean spoil disposal have reportedly increased the cost of dredging from $1 million to $15 million, in part due to court-ordered dredging requirements. The Port Authority has previously announced that it will construct a new $8.5 million on-dock rail terminal at its Port Elizabeth container facilities, which is scheduled for completion in the first quarter of 1995. Initial capacity of the facility will be 100,000 containers annually (WWS/World Wide Shipping, June 1994, p. 33).

Red Hook Container Terminal - Brooklyn, Howland Hook Container Terminal - Staten Island, NY. Red Hook terminal is the only marine cargo terminal still operating on the East side of the Harbor. It was reactivated in January 1994 under the management of American Stevedoring Ltd. The NY/NJ Port Authority is in the process of dredging the approach channel to its project depth of 11.6 m (38 ft). American Stevedoring anticipates handling 20,000 twenty-foot equivalent units in 1994 and as many as 70,000 twenty-foot equivalent units by 1995. The terminal also benefits from a Port Authority subsidized container-on-barge service connecting Red Hook with New Jersey railheads. Terminal facilities include 920 m (3,030 ft) of berthing, containers, roll-on/roll-off and breakbulk cargoes, rail service, four 36.3 metric ton (40 tons) container cranes, and one 63.7 metric ton (70 tons) container crane. While seeking an operator to revitalize the 58.7 ha (145 acre) Howland Hook container terminal—the former base of U.S. Lines idled since 1991, the Port Authority is completing a $25 million renovation of the terminal. Work includes replacement of electrical and distribution systems and resurfacing of a 762 m (2,500 ft) wharf. The Port Authority is also seeking a dredging permit to increase the depth of the berths from the original 10.1 m (33 ft) to the authorized depth of 12.2 m (40 ft). The terminal has a capacity of more than 300,000 containers a year. Its facilities include 762 m (2,500 ft) of lineal berthing space, four 36.3 metric ton (40 ton) and two 45.5 metric ton (50 ton) container cranes, and rail service (American Shipper, August 1994, Pages 73-74).

The City of New York – owner of the Terminal (Howland Hook), and the State of New Jersey are negotiating for the purchase of the Staten Island Railroad tracks between the Terminal and Cranford, NJ, where the short line

connects with Conrail. CSX owns the Staten Island line, but was granted approval in 1991 to abandon the route, so a new owner is needed to reactivate the rail line. City officials and the prospective operator of the Howland Hook facility predicted that the future of this terminal as a viable facility may hinge on the acquisition of the trackage and the installation of on-dock rail service (American Shipper, August 1994, p. 84).

Portland, OR

The Port Commission has approved a $60 million container terminal upgrade program for Terminal 6 to increase throughput capacity to 510,000 twenty-foot equivalent units over the next 10 years, nearly double its present capacity. The Terminal currently handles 314,500 twenty-foot equivalent units a year. Improvement plans include a new $16 million post-Panamax size container crane scheduled to come on stream by late 1995. The Port Commission has also hired an engineering consulting firm to recommend a development strategy and 20-year development program for a new marine terminal complex on West Hayden Island (*American Shipper*, October 1994, "Port of Portland Builds for the Future")

In July, the Port Of Portland Commission contracted with IBM and Stevedoring Services of America to provide the hardware and software for a new $1.0 million computerized terminal management system for its Terminal 6 container facility. The Port presently handles 600 trucks a day with a cargo inventory system developed in 1980. Portland is the fastest growing port on the West Coast (Containerization International, September 1994, "Portland Buys SSA System").

Portsmouth, VA

No immediate improvements identified.

San Francisco, CA

San Francisco's future as a leading West Coast container port is in jeopardy following the decision of Evergreen line to leave the port when its lease expires in June 1995. Evergreen's move follows the departure of Cosco, National Shipping Co. of the Philippines, Nedlloyd Line, Blue Star Lines, and South Seas Steamship. The anticipated reduction in revenues caused by these defections to the Port of Oakland may effect San Francisco's Port capital expenditure programs, including the $10 million rail tunnel improvement project designed to accommodate double-stack train services south of the City. Delays in executing this project are cited as the reason for the loss of these lines. The Port's North Container Terminal is presently dormant and the South Terminal is significantly under-utilized. As reported in WWS/World Wide Shipping, July/August 1994, Pg. 41: The Mayor of San Francisco announced a plan for a New Age entertainment center, incorporating a ballpark and a sports area to be built in space formerly used for cargo handling and Southern Pacific trackage—underscoring the trend to convert prime commercial waterfront land into resort and entertainment areas—an industry-wide problem (Containerization International, "San Franciscos Latest Setback," September 1994, p. 27).

Savannah, GA

Completion of a new 12.8 m (42 ft) shipping channel was completed this Spring. The 1.22 m (4 ft) deepening of the channel makes the Savannah terminals accessible to 98 percent of ships currently in the trade. 1994 is the

third year of Savannah's $319 million development program called *Focus 222*, which is designed to provide the facilities and infrastructure needed to maintain growth into the year 2000. Remaining elements of the Program include steps to help restore the freshwater habitat in the Savannah National Wildlife Refuge, completion of upgrading the 1,680 m (5,500 ft) of contiguous berth at Garden City's Container Berth 6, the addition of 12 ha (30 acres) of container storage and delivery of four new post-Panamax container cranes, two of which were scheduled to arrive late in 1994, and upgrading of existing container cranes, making a total of 13 container cranes at the Garden City port complex (WWS/World Wide Shipping, May 1994, p. 27).

Seattle, WA

The ports of Seattle and Tacoma use the findings of a 1990 econometric study sponsored by the Washington Public Ports Association as an integral part of their planning strategies. In the case of Seattle, this means being capable of handling 2.1-2.5 million twenty-foot equivalent units annually, 15 years hence. The port's Container Terminal Development Plan, adopted by the Seattle Port Commission in May 1991, called for another 97 ha (240 acres) of land to be developed by the end of the century. A further 41 ha (100 acres) has been scheduled for possible acquisition by the year 2010. Seattle currently has about 140 ha (350 acres) of land that is dedicated to container handling activities. The initial phase of the Program involves adding parking space, extending certain piers and upgrading shipside cargo handling gear. Additionally, the Container Terminal Development Plan calls for expansion of existing, and construction of new on-dock rail yards, and improving overall access to/from the port area. A summary of Seattle's current expansion/development programs includes:

a. Expansion of Terminal 5, operated by an affiliate of American President Lines, from 33.6 has to 64 ha (83 to 158 acres) and a 122 m (400 ft) extension of the berth. Work is scheduled for completion in 2 to 3 years;

b. An on-dock intermodal rail facility at Terminal 5 capable of handling two full-length double-stack rail cars simultaneously plus capacity for storing two more, and an overpass to segregate rail and truck traffic;

c. A 36.4 ha (90 acre) expansion to the 44.5 ha (110 acre) Terminal 18 located on the eastern side of Harbour Island. The expansion will permit doubling of the existing intermodal on-dock rail yard from 28 to 56 double-stack rail cars. The new south intermodal rail yard will have separate rail access to avoid conflict with Terminal 5 rail traffic. Container aprons will be upgraded, and the terminal's seven container cranes will be upgraded, and/or replaced by post-Panamax capacity gantry cranes. Additional plans call for an addition of 4 ha (10 acres) to the northernmost extremity of the Terminal, increasing its size to 18.2 ha (45 acres) and the lengthening of the ship berth by 122 m (400 ft). Terminal 18 is the Port's largest common-user facility, and will be able to handle two post-Panamax vessels at the same time (Containerization International, July 1994, pages 87-90).

Tacoma, WA

Tacoma's 20-year, $450 million 2010 Blair Waterway terminal expansion program is equally ambitious, but its implementation will be geared to customer demand. Major elements of the 2010 Blair Waterway program, which is designed to enable the waterway to handle the largest containerships afloat include:

a. The addition of approximately 125 ha (309 acres) of new container terminal area, 11 berths, and 30 ha (75 acres) of new intermodal rail facilities at the Port;

b. Dredging of the main access channel to a depth of 13.7 m (45 ft), and construction of a new city bypass road with subsequent dismantling of the Blair Road Bridge. The bridge is slated to be removed by the end of 1995 and the entire West Blair terminal project is to be completed by the end of 1996;

Additional planned port improvements include the construction of two new container terminals on the north side of the Blair waterway and the new terminals have two berths and 20.2 ha (50 acres) of land. The second new terminal will be built at the existing Terminal 7 and will consist of a one-berth 20.2 ha (50 acre) facility. Spoil from dredging work is being used to fill in the Milwaukee Channel and increase the Sea Land terminal by 9.7 ha (24 acres). According to the econometric study cited above, Tacoma will need to be able to handle between 2.5 and 2.8 million twenty-foot equivalent units in the year 2010 (Containerization International, July 1994, pages 87-90).

Wilmington, DE

No immediate improvements identified.

Wilmington, NC

Long term development plans by the North Carolina State Ports Authority include studies for the deepening of the outer bar channel to 14 m (46 ft), the river and harbor channel to 13.4 m (44 ft), and development of a new marine terminal upstream of the existing port complex. Dredging was expected to begin in early summer 1994 and site development work for the new terminal is slated for fiscal year 1996 provided funding is available. Similar planning for a new marine terminal on Radio Island, adjacent to existing port facilities at Morehead City, is underway. The recently completed channel and harbor dredging to 13.7 m (45 ft) makes Morehead City one of the deepest ports on the East Coast (WWS/World Wide Shipping, May 1994, p. 26).

Attachment D2
Port Population Growth Factors (1990 - 2010)

U.S. Ports	*Counties*	*1990*	*2010*	*Growth Factor*
		East Coast		
Boston, Massachusetts	Suffolk	663,906	792,200	
	Norfolk	616,087	631,300	
		1,279,993	1,423,500	1.11
Elizabeth, New Jersey	Essex	778,206	757,200	
	Kings, NY	2,369,966	2,364,992	
	Hudson	553,099	566,600	
	Richmond, NY	385,224	463,529	
	Union	493,819	502,300	
		4,580,314	4,654,621	1.02
Philadelphia, Pennsylvania	Philadelphia	1,585,577	1,513,674	
	Camden	502,824	550,500	
	Gloucester	230,082	269,300	
		2,318,483	2,333,474	1.01
Eddystone, Pennsylvania	Delaware	547,651	508,557	
	Philadelphia	1,585,577	1,434,694	
		2,133,228	1,943,251	0.91
Wilmington, Delaware	New Castle	441,946	513,750	
		441,946	513,750	1.16
Baltimore, Maryland	Baltimore	692,134	728,898	
	Anne Arundel	427,239	499,204	
	Howard	187,328	288,701	
		1,306,701	1,516,803	1.16
Newport News, Virginia	Isle of Wight	25,053	34,283	
	Norfolk City	261,229	253,809	
	Hampton City	133,793	146,648	
	York	42,422	56,000	
		462,497	490,740	1.06
Norfolk, Virginia	Isle of Wight	25,053	34,283	
	Norfolk City	261,229	253,809	
	Portsmouth City	103,907	101,965	
	Hampton City	133,793	146,648	
	York	42,422	56,000	
		566,404	592,705	1.05
Portsmouth, Virginia	Isle of Wight	25,053	34,283	
	Portsmouth City	103,907	101,965	
	Norfolk City	261,229	253,809	
		390,189	390,057	1.00
Wilmington, North Carolina	New Hanover	120,284	150,936	
	Brunswick	50,985	79,644	
		171,269	230,580	1.35
Charleston, South Carolina	Charleston	295,039	339,400	
	Berkeley	128,776	252,800	
		423,815	592,200	1.40
Savannah, Georgia	Chatham	216,935	273,391	
	Byran	15,438	23,610	
		232,373	297,001	1.28

U.S. Ports	Counties	1990	2010	Growth Factor
Fernandina Beach, Florida	Nassau	43,941	79,800	
		43,941	79,800	1.82
Jacksonville, Florida	Nassau	43,941	79,800	
	Duval	672,971	1,014,100	
		716,912	1,093,900	1.53
Port Everglades, Florida	Broward	1,255,488	1,980,900	
		1,255,488	1,980,900	1.58
Miami, Florida	Dade	1,937,094	2,809,700	
		1,937,094	2,809,700	1.45
		Gulf Coast		
Mobile, Alabama	Mobile	378,643	408,600	
	Baldwin	98,280	110,300	
		476,923	518,900	1.09
Gulfport, Mississippi	Harrison	165,365	175,291	
		165,365	175,291	1.06
Galveston, Texas	Galveston	217,399	245,820	
	Brazoria	191,707	249,644	
	Chambers	20,088	21,200	
		429,194	516,663	1.20
New Orleans, Louisiana	Jefferson	448,306	513,980	
	Orleans	496,938	514,740	
	St. Bernard	66,631	79,950	
	Plaquemines	25,575	29,820	
		1,037,450	1,138,490	1.10
		West Coast		
Seattle, Washington	King	1,507,319	1,833,133	
	Kitsap	189,731	261,970	
		1,697,050	2,095,103	1.23
Tacoma, Washington	Pierce	586,203	792,179	
		586,203	792,179	1.35
San Francisco, California	Marin	231,200	245,500	
	San Mateo	652,100	787,300	
	San Francisco	723,900	781,700	
		1,607,200	1,814,500	1.13
Concord Naval Weapons, California	Contra Costa	810,300	1,096,300	
	Solano	345,700	557,400	
		1,156,000	1,653,700	1.43
Oakland, California	Alameda	1,279,182	1,561,900	
	San Francisco	723,959	781,700	
		2,003,141	2,343,600	1.17
Los Angeles, California	Orange	2,424,100	3,104,100	
	Los Angeles	8,897,500	11,441,900	
		11,321,600	14,546,000	1.28
Long Beach, California	Orange	2,424,100	3,104,100	
	Los Angeles	8,897,500	11,441,900	
		11,321,600	14,546,000	1.28

+1990 Census taken from Rand McNally/The New Cosmopolitan World Atlas Census/Environmental Edition, 1992.

Alabama	Alabama Population Projections 1990-2015, Alabama State Data Center Center for Business and Economic Research, University of Alabama, Tuscaloosa, AL, January 1994.
California	Population Projections by Race/Ethnicity for California and its Counties, Report 93 P-1, Demographic Research Unit, Sacramento, CA, (916) 322-4651, April 1993.
Delaware	Census info and projection numbers through Evelyn Pearson, Delaware Development Office, Business Research Section, Dover, DE, Consortium Series, (302) 739-4271, June 30, 1994.
Florida	Projected from Florida Population Studies (by county) by Stanley K. Smith, Director, Bureau of Economic and Business Research, University of Florida, Volume 27/Number 2/Bulletin No. 108, February, 1994.
Georgia	Census info and projection numbers through Marty Sik, Governor's Office of Planning and Budget, Atlanta, GA, (404) 656-0911.
Louisiana	Census info and projections provided by Division of Administration, Baton Rouge, LA, Department of Budget, ATTN: ARL, (504) 342-7410.
Maryland	Department of State Planning, Office of State Planning Data, Office of Michael Lettre, , Baltimore, MD, (410) 225-4452, September 29, 1994.
Massachusetts	Ms. Alice Rarig, Massachusetts Inst. for Social & Econ Research (MISER), University of Mass., Amherst, MA, (413) 545-6660, September 30, 1994. **Calculations are only preliminary numbers. Final reports will be made available by end of October 1994.
Mississippi	Projections given by phone through the Office of Dr. Barbara Logue (EPA) on 9/29/94 from Center Policy Research & Planning, MS Institute of Higher Learning, Jackson, MS, (601) 982-6576, September 29, 1994.
New Jersey	Census info and projection numbers provided by Sen-Juan Wu, New Jersey Dept of Labor, Labor Market & Demographic Rsr, Trenton, NJ, (609) 292-0076.
New York	Census info and projections provided by New York State Bureau of Economic and Demographic Info, Albany, NY, (518) 474-6005.
North Carolina	Census info and projection numbers through Bill Tillman, Office of State Planning, Raleigh, NC, (919) 733-4131, Prepared April 1994.
Pennsylvania	Projections given by David Gordner, Bureau of Water Management, Department of Environmental Resources, Harrisburg, PA, (717) 772-4048, September 30, 1994.
South Carolina	Census info and projection numbers through Diana Tester, South Carolina Budget and Control Board, Office of Research & Statistical Services, Columbia, SC, (803) 734-3619, Published October 29, 1993.
Texas	Census info and projection numbers obtained through Texas State Data Center, Texas A & M University System, College Station, TX, 77843-2125, (409) 845-5115. Contact: Hazel Dolar.

Virginia	Projection given by Jeanne Brown, Center for Public Service University of Virginia, Charlottesville, VA, (804) 982-5580, September 28, 1994.
Washington	Census info and projections from Washington State County Population Projections, Office of Financial Management, Forecasting Division, Olympia, WA, January 31, 1992.

Attachment D3
Background Discussion of Alternative Analytical Models for Evaluation of Potentially Impacted Port Populations

In the Fall of 1993, the Department of Energy (DOE) began to collect and analyze information required for the list of port criteria included in the Notice of Intent (DOE, 1993) for this environmental impact statement (EIS). DOE recognized that there would be public concern associated with consideration of potential ports of entry for the foreign research reactor spent nuclear fuel. Therefore, DOE decided to develop a sound technical basis for the identification of potential ports of entry.

As a result (concurrently with the independent evolution of the Urgent Relief Environmental Assessment), a list of 28 potential commercial ports was established based on the recommendations of independent maritime consultants. The database included information in the following categories:

1. *Geophysical Factors*, harbor and channel water depths [a port would fail if it had less than 7 m (23 ft) of water, but receive the maximum score if it had more than the 12 m (40 ft) of water required for all but the largest cellular container vessels]; the nautical distance from the open ocean to the port [ports greater than 40 km (25 mi) from open ocean received no points, but were not disqualified from further consideration]; and navigational factors that might increase public risks (narrow, winding channels with currents or other factors seriously affecting safe navigation were given no points, but a weighting factor was applied to channels with good characteristics to account for the relatively greater importance of this factor for maritime safety).

2. *Port facilities*, which included the capabilities of cargo terminals for handling containerized foreign research reactor spent nuclear fuel, wharves and depths alongside, crane capacities, terminal access (truck and rail), terminal security, and the liner services available.

3. *Factors related to spent nuclear fuel handling and transport*, including past experience with spent nuclear fuel or other hazardous cargoes, whether there were local restrictions on the receipt of foreign research reactor spent nuclear fuel, emergency response capabilities, hazardous material handling training, locations of terminals relative to nearby populations with a doubleweighted score for ports that were remote from urban populations (e.g., heart of a city), 1990 census statistics for port city populations and population densities, environmental factors (whether the immediate port vicinity had sensitive populations of animals), and distance from the port to Savannah River Site and Idaho National Engineering Laboratory (at that time these were the preferred storage sites due to historical experience and facilities; the other three sites were added later as the result of the Programmatic Spent Fuel Draft EIS decision to consider them).

Using the database developed, a semi-quantitative analysis of the port criteria was prepared that summed the "score" assigned to each port attribute by the maritime experts, and the ports were ranked from best to the least acceptable (this list of ports is, for the most part, a subset of the set of over 40 ports that were subsequently analyzed in detail in Section D.2 of this appendix).

DOE determined that a semi-quantitative analysis of all ports for all of the noticed criteria was unacceptably subjective, especially concerning the assignment and weighting of the numerical scores. Furthermore, it did not differentiate well between ports, and when weighting factors were applied to better discriminate between criteria that were very important to safety versus those that were "desirable attributes," the methodology became very difficult to justify.

Attachment D4
Derivation of Ship Collision Damage Probabilities

Derivation of the accident severity category probabilities requires that a probability of damage to the transportation cask, given a collision between two vessels, be calculated. In Appendix D, this probability has been characterized by two values, P_{Impact} and P_{Crush}. The first is a probability that the cask is damaged due to impact forces associated with the collision. The second represents the probability that crush forces result in damage to the cask. This attachment describes how these probabilities were derived.

D4.1 Kinetic Energy

V.U. Minorsky developed a method for analyzing the collision of ships that provides a correlation between resistance to penetration and the energy absorbed in the collision (Minorsky, 1959). The absorbed energy was determined for actual collisions by assuming the impact was nearly transverse, the hydrodynamic forces due to water entrained by the hull of the struck ship could be treated as a virtual increase in mass, and the collision was perfectly inelastic. The resistance to penetration was quantified through a resistance factor, R_t, which was computed from accident and ship design information. He found, for higher energy incidents, that there is a linear correlation between R_t and the absorbed energy.

ORI Inc., in a draft report on accident severities associated with water transport of radioactive materials, extended Minorsky's method to develop correlations between penetration depth and the energy absorbed in ship collisions (ORI, 1981b). By considering empirical probability distributions for displacement of the striking ship, its speed, and the angle of impact, bounding case curves were developed for the probability of occurrence of force levels at selected penetration depths. The force value referred to is the collision force acting between the two ships.

Only a fraction the collision force would be seen by a spent fuel transportation cask on board the struck ship. ORI gave a qualitative discussion of this aspect of the collision, together with some limiting case values based on assumptions about stowage and the presence and type of other cargo.

The present analysis depends, to a large extent, on the Minorsky and ORI analyses. It does add an approximate treatment of accelerations experienced by the spent fuel package and includes the effects due to cargo in determining the maximum penetration depth in collision events. The dynamics of inelastic collisions are treated through conservation laws for momentum and energy. Following Minorsky, the transverse hydrodynamic forces on the hull of the struck ship are accounted for by a virtual increase in mass, hence kinetic energy. This is a conventional method used by naval architects, but has limitations when applied to collisions. M.J. Petersen pointed out that experiments and calculations by Motora et al., have shown that the added mass treatment is not always a good approximation (Petersen, 1982; Motora, 1971). Here we accept the limitations imposed by the added mass method, because a more rigorous treatment of the collision is not warranted due to other uncertainties in the analysis, particularly in the modeling of cargo effects.

It should be noted that the ORI/Minorsky method of calculating hull penetration probably does not take account of the massive keel structures in the struck transport ships. Therefore, they most likely significantly overestimate the probability of penetration further than one-fifth of the beam of the struck ship, since penetration to this distance would mean that the keel structures had been encountered. Note that historic experience (rule-of-thumb experience) indicates that few ship collisions lead to penetration more than one-fifth of the beam of the struck ship.

Parameters and Assumptions

The target ship in the following calculations is assumed to have a beam of 24.99 m (82 ft) and a displacement, 'm', of 25,310 metric tons (27,841 tons). The virtual mass, 'dm', due to hydrodynamic forces is 0.4 m = 10,120 metric tons (11,132 tons). Eight cases are considered for the displacement, 'm', of the striking ship: 5,600; 16,800; 28,000; 39,200; 50,400; 61,600; 72,800; and 84,000 metric tons (6,160; 18,480; 30,800; 43,120; 55,440; 67,760; 80,080; and 92,400 tons. The normal component of the striking speed at impact ranges from 1 to 10 meters per second (1.9 to 19 knots or 2.2 to 22 statute miles per hour).

A full distribution of sailing speeds (0-22 knots) was used in the penetration calculations even though speeds in port channels are likely to be no greater than 10-15 knots and speeds at dockside only a few knots (minimum required to maintain steerage). In addition, large ships (e.g., tankers) are likely to be pushed/towed by tugs near docks.

The models for energy absorption by the ship and its cargo follow the methods of ORI. The work, 'W', due to cargo compression is the product of the crush strength of the cargo, the cross sectional area of the blunted bow of the striking ship, and the difference between the penetration distance and the cargo closeup distance. ORI gave examples of this calculation, which are reproduced in the formula

$$W_{cargo} = 19.44 f \sigma \, (x - f(\,beam\,))$$

where f is the fraction of open space on the hold floor, σ is the crush strength of the cargo in MPa (mega pascals), 'x' is the penetration depth and beam is the width of the struck ship, both in meters. This formula follows ORI in assuming the vertical size of the damage zone is 7.62 m (25 ft), and one third of the blunted bow is the effective area.

Prior to the initiation of cargo compression, energy is absorbed solely by deformation of the ship structure; this effect is modeled using the Minorsky value of 32 'mj' (mega joules) for the energy to penetrate the hull, together with the semi-empirical curves in Figure 6.2 of the ORI report. Table D4-1 gives coefficients for a quadratic fit used to represent the ORI curves below 15 m (49.2 ft) penetration, while a second fit for greater penetration distances is given in Table D4-2.

Table D4-1 Quadratic Coefficients for Energy Absorbed Due to Ship Structures <15m

$$W_{ship} = a + bx + cx^2 \quad (x < 15m)$$

Metric ton	*a (mj)*	*b (mj/m)*	*c (mj/m^2)*
5,600	9.551	0.6836	0.0405
16,800	8.709	0.8118	0.2984
28,000	8.056	1.2030	0.4558
39,200	8.121	1.0850	0.5296
50,400	9.234	0.6555	0.6217
61,600	8.956	0.8639	0.6698
72,800	8.574	1.1790	0.6906
84,000	8.204	1.5290	0.7154

Table D4-2 Quadratic Coefficients for Energy Absorbed due to Ship Structures >15m

$W_{ship} = a + bx + cx^2$ (x >15m)

Metric ton	*a (mj)*	*b (mj/m)*	*c (mj/m^2)*
5,600	58.13	-4.837	0.1919
16,800	14.72	-0.057	0.3337
28,000	15.76	-0.304	0.5179
39,200	64.87	-5.622	0.7306
50,400	189.5	-19.21	1.162
61,600	264.4	-29.02	1.531
72,800	303.8	-36.36	1.878
84,000	412.2	-50.50	2.393

Distribution of Ship Displacements, Speeds and Angles

Analysis of two years of shipping accident data allowed ORI to develop probability distributions for 'M' (mass of the striking ship), 'V' (transverse speed of the striking ship), and θ (angle of incidence), which are presented here in Table D4-3 through D4-5. The ORI tables originally contained eleven intervals for displacement of the striking ship. Four cargo loadings were examined in the analysis: no cargo, light cargo, medium cargo, and heavy cargo (light, medium, and heavy refer to the amount of cargo on board). For the present work, the two lowest intervals were combined as were the three highest, yielding eight intervals to match the eight ORI curves for 'W'. There were also 11 values of 'V' in the ORI tables, with speeds ranging up to 11.3 meters per second (21.5 knots or 24.9 statute miles per hour), and 9 values of the collision angle. Thus 968 different combinations of these values are treated in determining transportation cask failure.

Table D4-3 Probabilities for Striking Ship Displacement

Displacement (metric ton)	*Probability of Occurrence*
0 - 10,160	0.15
10,161 - 20,321	0.25
20,322 - 30,481	0.25
30,482 - 40,642	0.05
40,643 - 50,802	0.05
50,803 - 60,963	0.05
60,964 - 71,123	0.10
71,124 - 152,407+	0.10

Table D4-4 Probabilities of Striking Ship Speeds

Speed (meters/second)[a]	*Probability of Occurrence*
0.0 - 1.028	0.0448
1.028 - 2.058	0.2538
2.058 - 3.087	0.1045
3.087 - 4.115	0.1343
4.115 - 5.144	0.1343
5.144 - 6.173	0.0896
6.173 - 7.202	0.0746
7.202 - 8.231	0.0597
8.231 - 9.260	0.0746
9.260 - 10.29	0.0149
10.29 - 11.32	0.0149

[a] *1 meters per second = 1.9 knots = 2.2 miles per hour*

Table D4-5 Probabilities of Striking Ship Angles of Incidence

Angle From the Normal (degrees)	*Probability of Occurrence*
0 - 10	0.2754
10 - 20	0.1305
20 - 30	0.0725
30 - 40	0.1305
40 - 50	0.1015
50 - 60	0.0724
60 - 70	0.1303
70 - 80	0.0435
80 - 90	0.0434

Speed During a Collision

In the following, 'M' and 'V' are the mass and transverse speed of the striking ship, while 'm' and 'v' denote the mass and transverse speed of the struck ship. Theta (θ) is the angle of impact, measured from the normal to the direction of the struck ship (this is the angle used by ORI, Minorsky and Petersen use its complement). The amount of virtual mass attributed to the struck ship to account for transverse hydrodynamic forces is 'dm'. W(x) denotes the work done in deforming the ships and compressing the cargo during a penetration to a depth 'x', and E_0 is the initial kinetic energy in the motion of the striking ship transverse to the struck ship.

The total energy in the transverse motion of the striking ship is:

$$E = MV^2 \cos^2(\theta)/2$$

Because energy is conserved during the collision, and neglecting turning effects,

$$E = \frac{MV^2}{2} + \frac{(m+dm)\,v^2}{2} + W(x)$$

Because momentum is conserved,

$$MV\cos(\theta) = MV + (m+dm)\,v$$

Together these equations yield a quadratic expression of the velocity of the struck ship:

$$\frac{Av^2}{2} - V\cos(\theta)\,v + \frac{W(x)}{m+dm} = 0$$

where A = (1+(m+dm)/M).

The value of the struck ship's transverse speed during the collision is, therefore,

$$v = \frac{V\cos(\theta)}{A} - \frac{1}{A}\sqrt{V^2\cos^2(\theta) - \frac{2AW(x)}{m+dm}}$$

The second term in this equation decreases to zero during the collision, yielding a terminal speed of $V\cos(\theta)/A$. This is also the terminal speed component of the striking ship in the same direction. The change in kinetic energy is (1-1/A)E = (m+dm)/(M+m+dm)E, in agreement with Minorsky.

Maximum Penetration Distance

The maximum penetration of the bow of the striking ship into the target ship was computed by finding, using Newton's method, the position at which the ships reached their terminal speed. From the conservation laws for energy and momentum, the condition for this to occur is:

$$0.5\,\mu\,V^2\cos^2(\theta) = W(x)$$

where $\mu = M(m+dm)/(M+m+dm)$, and $V_{\cos(\theta)}$ is the initial normal speed of the striking ship. For the no cargo case, it was found that for each of the striking ship displacements considered, initial normal speeds of 8 meters per second (15.2 knots or 17.6 statute miles per hour) and 10 meters per second (19.0 knots or 22.0 statute miles per hour) were sufficient to cut completely through the struck ship, resulting in a probable sinking; refer to Figure D4-1. On the other hand, at 2 meters per second (3.8 knots or 4.4 statute miles per hour) only the four heavier ships would even penetrate the hull of the struck ship, and at or below 1 meters per second (1.9 knots or 2.2 statute miles per hour) the hull was not punctured for striking ships of any displacement.

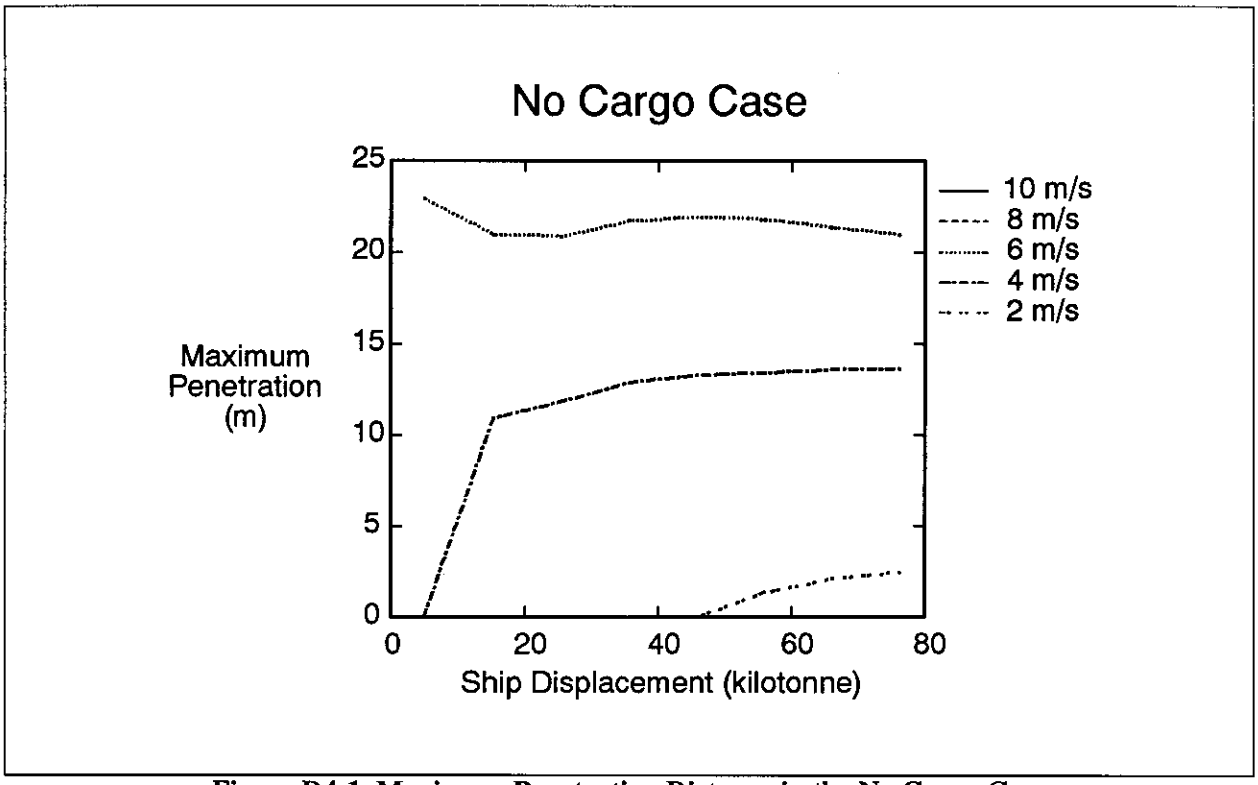

Figure D4-1 Maximum Penetration Distance in the No Cargo Case

Figure D4-2 shows the corresponding information for the light cargo case. Because of the packing fraction for this case, 0.6, the cargo effect does not begin until penetration has reached 15 m (49.2 ft). The figure shows the results as a function of the displacement of the striking ship, for normal impact speeds from 2 meters per second (3.8 knots or 4.4 statute miles per hour) to 10 meters per second (19.0 knots or 22.0 statute miles per hour). There were no cases where the struck ship would be completely cut through. At the two lower speeds, the cargo did not close up, hence was not a factor in absorbing the impact energy. There was no penetration at 1 meter per second (1.9 knots or 2.2 statute miles per hour) for any of the eight striking ship displacements considered.

The medium and heavy cargo results are shown in Figures D4-3 and D4-4, respectively. Figure D4-3 shows the cargo effect beginning at 5 m of penetration, and is important down to impact speeds of 4 meters per second (7.6 knots or 8.8 statute miles per hour). The cargo did not close up at smaller speeds, so was not a factor in determining the penetration depths. A similar result was obtained for heavy cargo; in both cases there was a strong influence by the cargo on the maximum penetration depth.

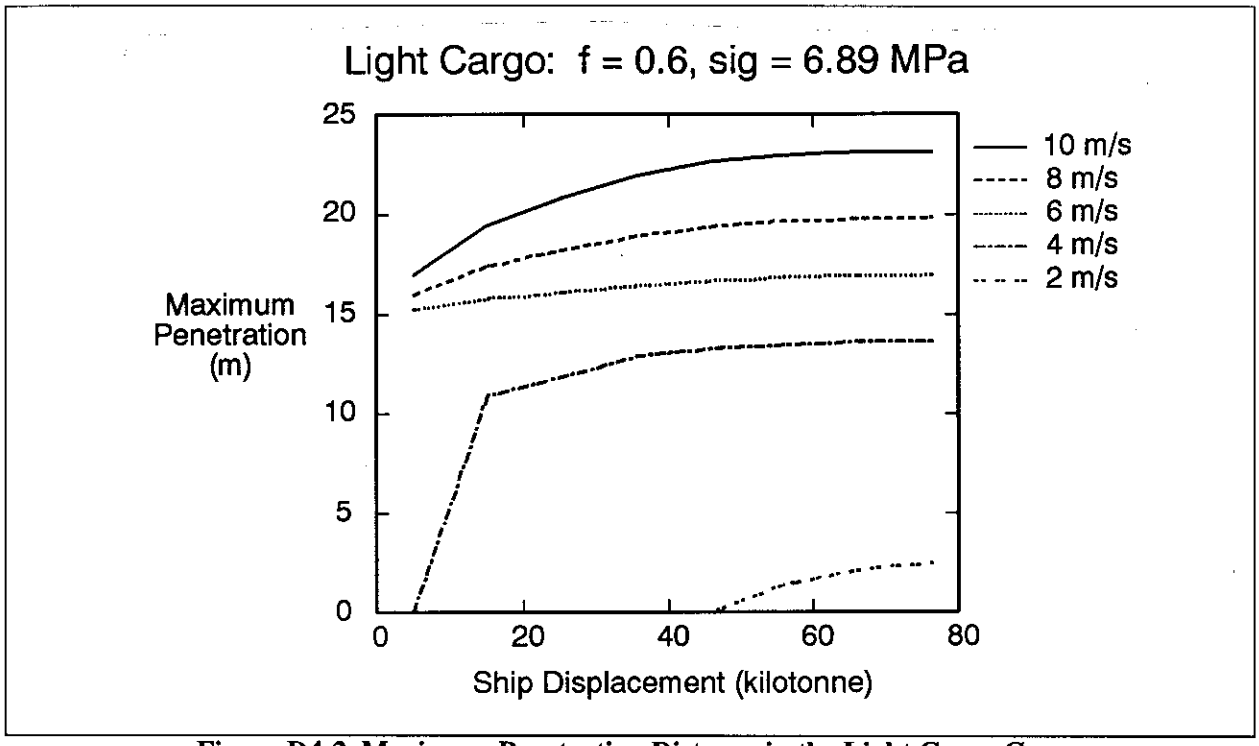

Figure D4-2 Maximum Penetration Distance in the Light Cargo Case

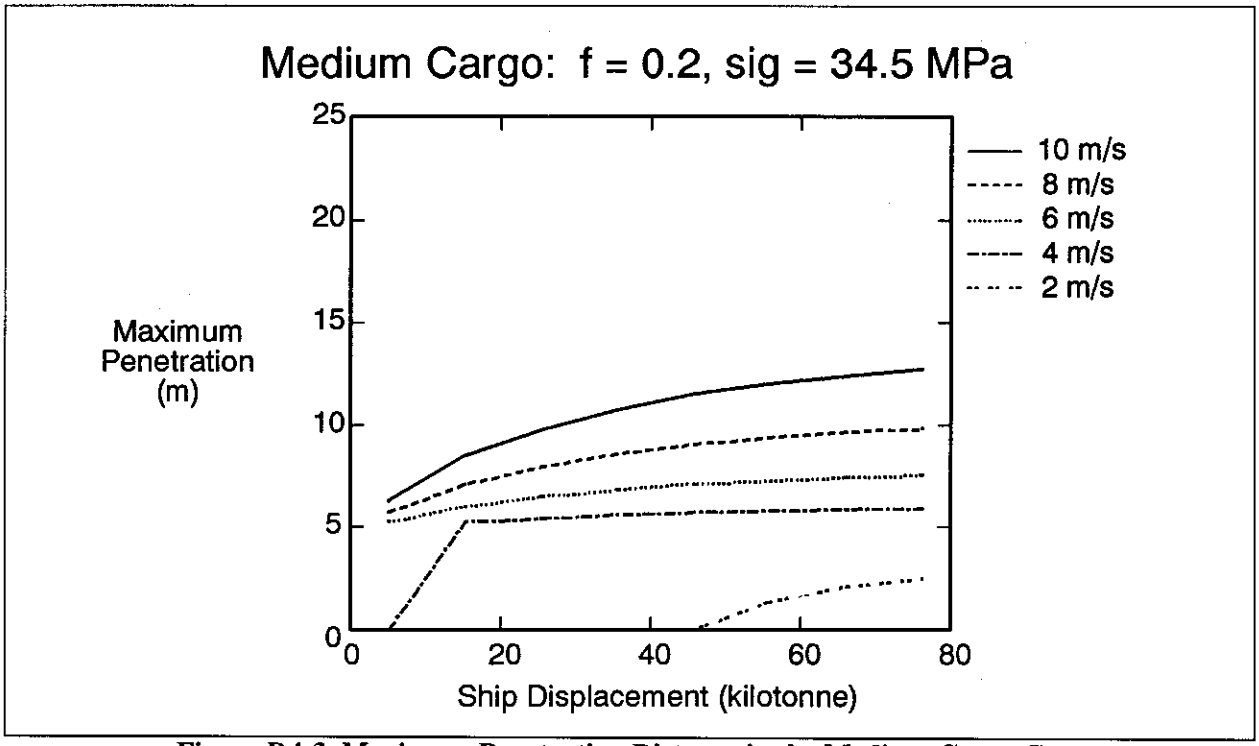

Figure D4-3 Maximum Penetration Distance in the Medium Cargo Case

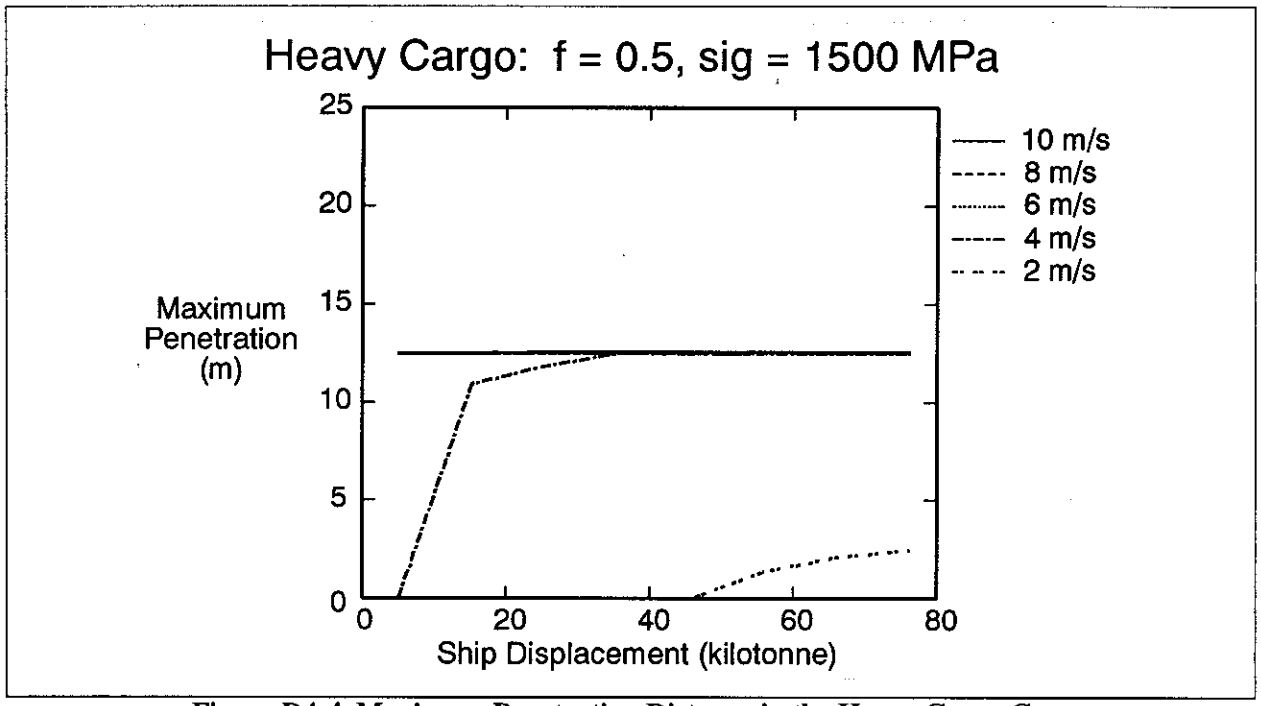

Figure D4-4 Maximum Penetration Distance in the Heavy Cargo Case

D4.2 Impact Forces During the Collision

Fuel elements experience impact forces if during a strong acceleration event they are driven against the inside of the cask or basket, or come into hard element to element contact. It is shown in Sanders et al., (Sanders, 1992) that accelerations of 100 g can be produced in the hypothetical accident conditions defined by NRC, which involve 9-m (29.5-ft) drops onto unyielding targets (NRC, 1990). They also showed there is a resulting cladding breach probability that for some power fuel types can be up to 0.0002 per rod in such events. We show here that the average acceleration experienced in ship collisions is very much smaller, usually below 1g, and conclude that inertial effects on the fuel are not significant for ship collisions.

The acceleration as a result of a ship collision is the time derivative of the transverse speed of the struck ship:

$$a = \frac{dv}{dt} = \frac{dv}{dx}\frac{dx}{dt} = v\frac{dv}{dx}$$

Performing the derivatives yields:

$$a = \frac{v(x)\,F(x)/(m+dm)}{\sqrt{V^2\cos^2(\theta) - \frac{2A\,W(x)}{m+dm}}}$$

where F(x) = dW(x)/dx. Notice that the acceleration peaks at the end of the collision, because the argument of the square root goes to zero there. The acceleration has a vertical asymptote at the maximum distance of penetration; the average acceleration, however, remains small.

The average acceleration during the collision is:

$$\langle a \rangle = \frac{\int_o^d a(x)dx}{d} = \frac{V^2 \cos^2(\theta)}{2\,d\,A^2}$$

where d is the maximum penetration depth. This is an improper integral since a (x) has a singularity at 'd'. However, the integrand increases sufficiently slowly in the neighborhood of 'd', like $(x-d)^{-1/2}$, for the integral to converge.

When there is no other cargo in the hold with the spent fuel cask, the average acceleration is only a fraction of 1g (9.8 meters per second^2) in all cases, with the average acceleration always less than 5 meters per second^2. Similar results hold for the light and medium cargo cases. Even in the extreme case of heavy cargo, the average accelerations found were less than 2.5g. The highest acceleration, corresponding to a 75,000 metric tons (82,500 ton) ship striking with a normal speed of 10 meters per second (19.0 knots or 22.0 statute miles per hour), was about 0.2g (2 meters per second^2).

Because of these low average accelerations, generally on the order 1 percent relative to the accelerations expected in the NRC regulatory accident conditions, impact of fuel elements inside the cask is not expected to do any damage to the fuel as a result of collisions either in port or on the high seas. We conclude $P_{impact} = 0.0$.

D4.3 Crush Loads on the Fuel Package During the Collision

The spent fuel package of interest is the Pegase transportation cask, a cask of french design. It is a lead shielded cask, with a mass of 18.9 metric tons (20.8 ton), a diameter of 1.875 m (6.2 ft), and a height of 2.239 m (7.3 ft). It has a body composed of two stainless steel shells built around a lead shield. It is designed to carry fuel or other radioactive material in baskets of differing design which fit into the cylindrical cavity of the cask. A detailed analysis of the mechanical response of the Pegase transportation cask to crush forces is not available, however it is similar in construction to the lead shielded cask analyzed in the study of Fischer et al., (1987).

Fischer et al., developed a curve for the static force versus deflection for sidewise loading of a cask which was 4.9 m (16.1 ft) high, with a lead shield 0.133 m (0.4 ft) thick enclosed by an outer layer of stainless steel 0.0318 m 1.25 in) thick and an inner layer 0.0127 m (0.5 in) thick. Because a Pegase transportation cask is much shorter, but of similar construction, it will be at least as resistant to sidewise loading as Fisher's generic lead shielded cask. Fisher's results show that it requires a load of about 8.9 million newtons to produce a deflection of the cask body of 0.0254 m (1 in). A deflection of 0.0254 m (1 in) is judged to be a conservative deflection that could occur without damage to the fuel. Said another way, sidewise cask loading on a Pegase transportation cask in excess of 8.9 million newtons would probably result in some disruption of the fuel. Now the questions is, can crush forces on the cask as high as 8.9 million newtons be produced in a ship collision? To the extent that the homogeneous cargo models are applicable, the answer is "yes." The force applied by the cargo in these models, after closeup, is a constant equal to:

$$F_{cargo} = \sigma\, hd$$

where σ is the cargo crush strength, and 'hd' is the cross sectional area of the cask; for the Pegase transportation cask, 'hd' is 4.198 m^2 (45.2ft^2). Thus, the force in the light cargo case is 56.0 million newtons, and for the medium and heavy cargo cases it is many times larger. These values so far exceed the damage threshold at 8.9 million Newtons that major damage to the fuel and cask can be expected.

But if the cargo does not close up because the penetration is shallow or there is no other cargo in the hold, the cask does not see this force. Then, unless it is within the penetration region, it will not be significantly affected.

Inside the penetration region the cask can be crushed without the cargo going solid, or even if there is no other cargo in the struck hold. Cask tiedowns are designed, under U.S. regulatory practice, to withstand about 5 million newtons of transverse force (NRC, 1990). The difference between this value and the 8.9 million newtons required to produce a 0.025 m (1.0 in) deflection in the cask wall of the generic cask is not considered significant; moreover in ORI's opinion "the RAM [Radioactive Material] package could conceivably be restrained from sliding, even in an empty hold, after the fittings failed. A buckled deck for example could do this and in effect act as an infinitely strong fitting" (ORI, 1981a).

Thus there are two cases to consider for failure due to crush forces. In the first the penetration depth exceeds the cargo close-up distance, while in the second it exceeds the cask stowage location. We assume fuel damage and closure failure in both types of events.

Cask Failure Probability

This section evaluates the probability that a cask will fail when the ship carrying it is struck in a collision with another ship. Since there are two different scenarios, the total probability of cask failure is the sum of two terms, one of cargo going solid, the other for the ship over-running the cask location, or

$$P_{\text{crush}} = P_{\text{solid}} + P_{\text{contact}}.$$

P_{solid} and P_{contact} were evaluated by comparing the maximum penetration distance against the closeup distance and the stowage position, assumed to be on the centerline of the hull, for all combinations of striking ship displacement, speed, and angle given in Tables D4-3 to D4-5. Each individual case was counted as either resulting in cask failure (meaning the fuel is damaged and the cask seal is broken) or not, and the probability of the case was assigned according to the probability values in the referenced tables. The sum $P_{\text{solid}} + P_{\text{contact}}$ of the probabilities of all failure cases is P_{crush}.

The results are shown in Figure D4-5. The successive columns refer to the four models considered, for no cargo, and light, medium and heavy cargo. For other than the medium cargo model, the total crush probability is about 0.29, although the fraction due to the cargo going solid varies from 0 for the no cargo case to 1 for the heavy cargo case. The medium case, which as the smallest fraction of open hold space at 0.2, also has the highest failure rate, about 0.45. Of the four cases considered, this is the only case where the cargo goes solid well before the midline of the ship is reached, thus permitting a greater proportion of all the collisions to be significant from a cask damage point of view. Since this case shows the greatest probability, it is conservative to take $P_{\text{crush}} = 0.45$.

Alternate Case

Because the top speed in a harbor is controlled, the ORI distribution was adjusted to a top speed of 8.23 meters per second (15.6 knots or 18.1 statute miles per hour). This reduced the number of speed intervals to eight, and eliminated the three highest speed categories in Table D4-4. The total number of combinations of striking ship displacement, speed, and angle was therefore reduced from 968 to 704. Figure D4-6 shows the revised cask failure probabilities for the four cases. The highest failure probability is still from the medium cargo case, probably because this case has the earliest cargo closeup distance and fails most often from collisions which do not penetrate far into the target ship. The failure probability goes down more in the other cases because they involve penetrations going past the midline of the ship. Such events are sensitive to the high end of the speed distribution. The cask crush probability for this alternative is set equal to the largest result, $P_{\text{crush}} = 0.40$.

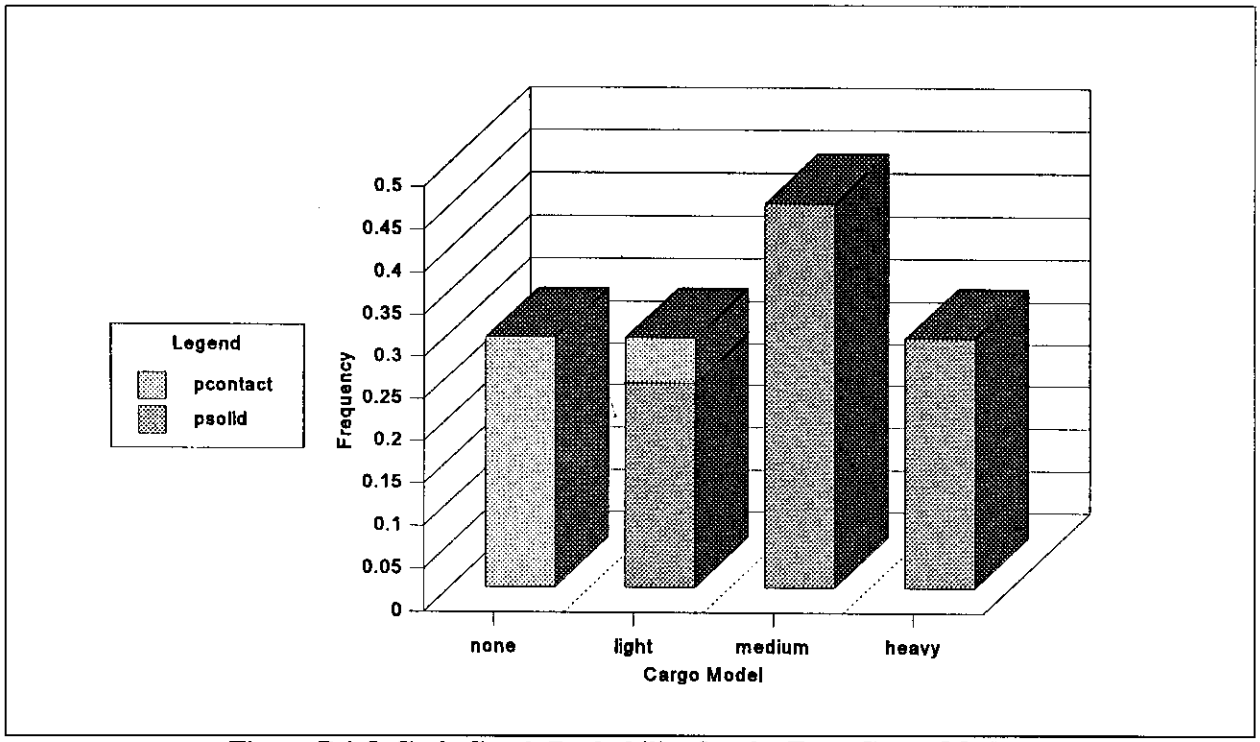

Figure D4-5 Cask Crush Probability for the Four Cargo Models

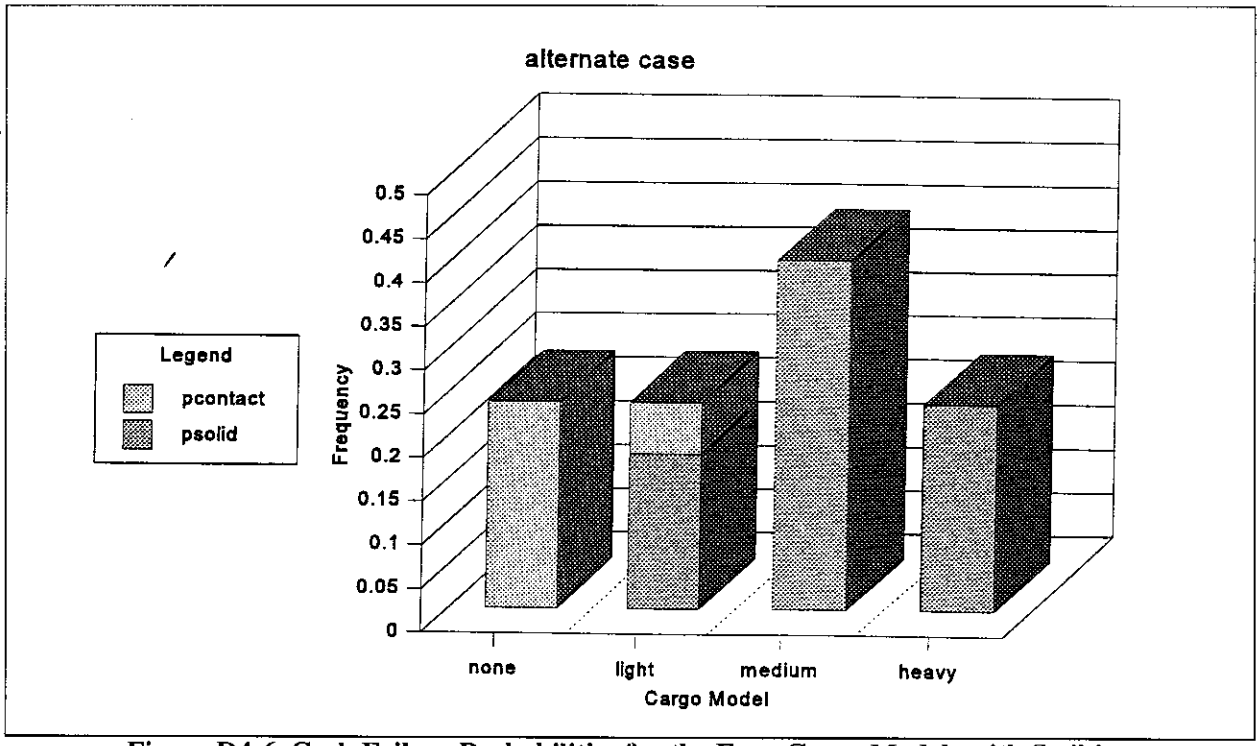

Figure D4-6 Cask Failure Probabilities for the Four Cargo Models with Striking Ship Speeds Truncated at 8.23 m/s

Attachment D5
High Temperature Effects on Research Reactor Fuel Release Fractions

D5.1 Introduction

Previous assessments of the accident risks associated with the transport of research reactor fuel did not specifically address certain high temperature (somewhat above 900°K or 1160°F) effects on the fuel. In this temperature range, aluminum based fuels (the aluminum-uranium alloys used in research reactor fuels) are susceptible to melting. Additionally, TRIGA fuel is spontaneously combustible in this same temperature range, if sufficient oxygen is available. The melting point for the uranium dioxide fuels that had been used as the basis for the development of estimates of the release fractions for earlier assessments is considerably higher than for the aluminum based fuels. These earlier assessments were the basis for the release fractions used in the base case analysis of this study. This attachment provides an assessment of the impact of these high temperature effects on the release fractions, and the probabilities of the accident severity categories, used in the base case study. This assessment forms the basis for the sensitivity study provided in Section 5.4.3.2 of Appendix D.

D5.2 Fission Product Release At High Temperatures

Table D-21 shows that accident severity category 4 accidents are caused by a ship collision that fails the seal of the spent fuel transport cask; that category 5 accidents add a severe engulfing fire to the conditions that characterize category 4 accidents; and that category 6 accidents assume an engulfing fire and a more severe cask failure (one medium sized hole or two or more small holes), one that allows the severe fire to induce substantial convective flow of air through the failed cask. Table D-21 also shows that the principal difference between severity category 5 and severity category 4 release fractions is a five order-of-magnitude increase (from 1.0×10^{-8} to 9.0×10^{-4}) in the release fraction for cesium; and that the principal difference between severity category 6 and severity category 5 release fractions is a 42-fold increase (from 1.0×10^{-6} to 4.2×10^{-5}) in the release fraction for ruthenium.

Much increased cesium volatility at the elevated temperatures to which the spent fuel is heated by the severe fire is the cause of the five order-of-magnitude increase in cesium release assumed for category 5 accidents. Conversion of elemental ruthenium to volatile ruthenium oxide (RuO_4) by oxygen, due to convective air flow through the failed cask, is the cause of the 40 fold increase of ruthenium release assumed for category 6 accidents.

The release fractions listed in Table D-21 and used in the base case analysis were constructed from release estimates developed (Wilmot, 1981; Wilmot et al., 1981) for power reactor fuel (uranium dioxide pellets clad in zircaloy). The fuels used in research reactors are not uranium dioxide pellets clad in zircaloy. TRIGA reactors use large pellets formed from a mixture of uranium, zirconium, and zirconium hydride (ZrH_2) that are clad in stainless steel. All of the other reactors considered in this assessment (BR-2 and RHF) use aluminum-clad metallic fuels where the metal is an alloy of aluminum and uranium (Al-U). At elevated temperatures (above 900°K or 1,160°F) these fuels melt and, if exposed to air, TRIGA fuel burns. Therefore, if a ship collision leads to a fire that heats these fuels to temperatures much above 900°K (1,160°F), fission product releases from these fuels will differ markedly from that predicted for uranium dioxide power reactor fuels. Therefore, the properties of metallic aluminum-uranium alloy fuels and of TRIGA fuel were reviewed to identify any significant differences between releases from these fuels and releases from power reactor fuel when these fuels are heated to elevated temperatures.

The BR-2, and RHF fuels considered by this study are fabricated as stacks of aluminum-uranium alloy plates or cylinders that are contained in aluminum-cladding. Release of fission products from aluminum-uranium alloy fuels has been reviewed (Ellison, 1993). Fission product release is minor below about 923°K (1,202°F), the melting point of the aluminum-uranium alloy from which these fuels are fabricated. Once the aluminum-uranium alloy has melted, fission products volatile at melt temperatures are rapidly released to the gas space above the molten alloy. Although molten aluminum can dissolve both the stainless steel spacers that support individual fuel bundles and the alloy fuel plates, melting of the aluminum-cladding that surrounds these alloy fuels does not significantly affect release because the melting temperature of the clad, 933°K (1,220°F), is slightly higher than the melting temperature of the alloy fuel.

The effects of air ingression on the release of fission products from commercial reactor fuel have been reviewed (Powers, 1994). That review indicates that ruthenium release fractions from uranium dioxide fuel will equal or exceed 4.2×10^{-5}, the release fraction for ruthenium used in the base case analysis for category 6 accidents, if the fuel is exposed to air for 15 to 30 minutes while heated to 700°K (800°F). The review also indicates that release increases rapidly as temperature rises or exposure times lengthen, and that for temperatures less than 1,200°K (1,700°F), ruthenium is released principally as ruthenium-oxide.

TRIGA fuel is a uranium-zirconium-hydrogen alloy that burns spontaneously in air at temperatures above 925°K or 1,205°F (Benedict, 1981). Because this combustion process is highly exothermic, if a severe fire heats a failed cask containing TRIGA spent nuclear fuel to temperatures above 925°K (1,205°F), air ingression due to convection or contraction of cask gases upon cask cooling would be expected to initiate spontaneous combustion of the fuel alloy, which should lead to substantially increased release from the fuel to the cask interior of krypton, cesium (most likely as cesium hydroxide, CsOH), and ruthenium [by conversion to volatile ruthenium oxide (RuO_4)].

Theoretical (NRC, 1988; SNL, 1989; GNS, 1993; Shaffer, 1994) and experimental (Babrauskas, 1986b; Nelsen, 1986; Gregory, 1987; Gregory, 1989; Schneider, 1989; Keltner, 1994) estimates of the thermal loads on casks produced by engulfing fires indicate that only engulfing fires with durations of an hour or more caused by the combustion of high-grade fuels (gasoline, jet fuel, diesel fuel) with an ample oxygen supply can raise the spent fuel contained in the casks to temperatures that approach 1,000°K (1,340°F). These studies also indicate that cask temperatures this high are not attained for fires of similar duration caused by poorer fuels (e.g., crude oil, wood). Thus, short duration fires involving low-grade fuels or mixtures of low and high-grade fuels are unlikely to raise cask temperatures high enough to significantly increase cesium vaporization or to cause substantial conversion of ruthenium to volatile ruthenium oxide. Fires involving high-grade fuels that are oxygen-starved because hold covers are closed or suppressed by the operation of fire fighting systems are also unlikely to result in elevated release fractions. Conversely, engulfing fires of about one hour duration that involve high-grade fuels could, for some accidents, be able to heat cask interiors to temperatures where (1) aluminum-uranium alloy fuels melt, (2) krypton, cesium, and ruthenium are easily vaporized, both from TRIGA fuel pellets and from melted aluminum-uranium alloy fuels, and (3) conversion of ruthenium to ruthenium oxide is substantial, if either fuel is exposed to air. The impact of these high temperature affects on the accident severity category 5 and 6 release fractions are discussed in the following paragraphs.

Accident Severity Category 5

When fuel temperatures remain below 900°K (1,160°F), that is, below the ignition point of TRIGA fuel in air and the melting point of aluminum-uranium alloy fuels, the release fractions from TRIGA fuel should be similar to that from uranium dioxide fuels. Also, the releases from aluminum-uranium alloy fuels should be very small, perhaps negligible, since diffusion in the metal plates from which the fuel is fabricated will be too slow to cause significant release to the cask, much less to the environment.

When research reactor fuels are heated significantly above 900°K (1,160°F) the release to the cask from TRIGA fuel pellets and from melted aluminum-uranium alloy fuels of krypton, volatile cesium, and ruthenium should be substantial (Cubicoitti, 1984; Cordfunke, 1990). Once released to the cask interior, transport of these fission products from the cask to the environment (past the failed cask seal) will only be efficient when the gases in the cask expand significantly due to heating of the cask to temperatures well above 900°K (1,160°F). For example, if melting of an aluminum-uranium alloy fuel at 923°K (1,202°F) causes essentially all of the krypton trapped in the fuel to be released to the cask interior, then further heating of cask gases to 1,023°K (1,382°F) by the fire will cause approximately 10 percent of the gases in the cask, including the krypton that escaped from the fuel to the cask interior, to be lost to the environment by expansion past the failed cask seal.

After the fire dies out, cooling of the hot cask will cause air to be drawn into the cask as the gases in the cask cool and contract. Thus, almost any hot fire of substantial duration will lead to substantial air ingression into a failed cask. Enhanced ruthenium release will then occur only if large amounts of fuel are exposed to the air, if this exposure occurs when the fuel is still hot enough to allow ruthenium to be oxidized to a volatile species, and if there is a transport process operating that causes the volatile ruthenium species to be released from the failed cask.

Because aluminum-uranium alloy fuels are molten at temperatures above 923°K (1,202°F), after air is drawn into the cask by cooling, if still molten, substantial exposure of fuel to air will occur, and therefore oxidation of ruthenium to ruthenium oxide will occur. However, after release to the cask interior, release of ruthenium to the environment can only occur by an inefficient transport mechanism, diffusion against the inflow of air since the cask is now cooling down. Thus, category 5 accident conditions, even those that reach unusually high temperatures, are not expected to significantly increase ruthenium release from aluminum-uranium alloy fuels, unless after dying down and drawing air into the cask, the fire flares up anew and again heats the cask to elevated temperatures whereupon gas expansion would transport some of the oxidized ruthenium vapors from the cask to the environment.

Because TRIGA fuel burns spontaneously and exothermically at temperatures above 900°K (1,160°F), if cask cooling draws air into a cask that contains TRIGA fuel while the fuel is still at such elevated temperatures, fuel burning will convert ruthenium to ruthenium oxide, and heating of the fuel and the cask gases by the highly exothermic oxidation of the hydride fuel will cause the oxidized ruthenium to vaporize, the cask gases to expand, and some of the vapors to be transported from the cask to the environment.

Accident Severity Category 6

During category 6 accidents, release from fuel to the cask interior of krypton, cesium, and ruthenium (after conversion to ruthenium oxide by exposure to air), occurs by the same processes that were just discussed for category 5 accidents. Gas convection through the failed cask is, by definition, substantial during category 6 accidents. Exposure of hot fuel to air causes substantial conversion of ruthenium to ruthenium oxide. Additionally, all vapors released from the fuel to the cask are transported from the cask to the environment by the convective flow of gases.

D5.3 Release Fractions for High-Temperature Events

The discussion presented in Section D5.2 indicates that, at elevated temperatures, release fractions for aluminum-uranium alloy and TRIGA fuels will differ substantially from those assumed in earlier studies of research reactor fuel transportation accidents for category 6 events and also for category 5 events that reach unusually high temperatures. To allow the consequences of such high-temperature events to be examined, the severity category strategy used in the base case analysis was modified by dividing both categories 5 and 6 into a low temperature and a high temperature category. Release fractions were then estimated for all of the categories in the modified strategy (categories 4, 5A and 5B, and 6A and 6B) and sensitivity calculations were performed to estimate the effects of the new release fractions on accident consequences.

Fire events that do not heat cask contents above 900°K (1,160°F) are placed in categories 5A and 6A. Fire events that heat cask contents above 900°K (1,160°F) are placed in categories 5B and 6B. Events that lead to seal failure are placed in category 4 and 5. Events that lead to cask failures (one medium hole, two or more small holes) that allow significant convective flow of gases through the failed cask are placed in category 6. Thus, transport of fission products released from fuel to the cask interior for category 5 events must be driven by expansion of cask gases due to heating of the cask by the fire, while for category 6 events, transport from the cask to the environments is efficiently driven by convective flow of gases through the cask. Table D5-1 summarizes the attributes of the modified severity categories.

Table D5-1 Category Attributes for the Modified Release Category Strategy

Category	*Cask Failure Mode*	*Transport from Cask*	*Temperature of Cask Contents*
5A	Seal Failure	Gas Expansion	T < 900°K
5B	Seal Failure	Gas Expansion	T > 900°K
6A	One medium hole, two small holes	Convection	T < 900°K
6B	One medium hole, two small holes	Convection	T > 900°K

Table D5-2 presents the release fractions developed for this modified strategy. Summarized in the footnotes of Table D5-2 are the basis for these release fractions. This table also compares the revised release fractions to the release fractions that were used in all of the base case calculations performed in this study. The sensitivity calculations that were performed using these new release fraction are described in Appendix D Section 5.4.3.2.

Table D5-2 Modified Release Fractions for Severity Categories 4, 5, and 6

Severity Category	*Study*	*Fuel*	*Chemical Element Group*			
			Krypton	*Cesium*	*Ruthenium*	*Particulate*
4	Base Case	Both	0.01	1.0x10-8	$1.0x10^{-8}$	$1.0x10^{-8}$
	Sensitivity Case	TRIGA	0.1	1.0x10-7	$1.0x10^{-7}$	$1.0x10^{-7}$
		Aluminum-uranium	$1.0x10^{-8}$	$1.0x10^{-8}$	$1.0x10^{-8}$	$1.0x10^{-8}$
5	Base Case	Both	0.1	$9.0x10^{-4}$	$1.0x10^{-6}$	$5.0x10^{-8}$
5A	Sensitivity Case	TRIGA	0.26	$1.0x10^{-3}$	$2.3x10^{-6}$	$1.3x10^{-6}$
		Aluminum-uranium	$1.3x10^{-7}$	$1.3x10^{-7}$	$1.3x10^{-7}$	$1.3x10^{-7}$
5B	Sensitivity Case	TRIGA	0.31	$1.1x10^{-2}$	$9.8x10^{-3}$	$3.3x10^{-4}$
		Aluminum-uranium	0.098	$9.8x10^{-3}$	$1.7x10^{-6}$	$3.0x10^{-7}$
6	Base Case	Both	0.11	$9.8x10^{-4}$	$4.2x10^{-5}$	$5.0x10^{-8}$
6A	Sensitivity Case	TRIGA	0.35	$1.6x10^{-3}$	$3.6x10^{-6}$	$2.0x10^{-6}$
		Aluminum-uranium	2.0x10-7	$2.0x10^{-7}$	$2.0x10^{-7}$	$2.0x10^{-7}$
6B	Sensitivity Case	TRIGA	1.0	0.3	0.3	0.01
		Aluminum-uranium	1.0	0.1	$1.6x10^{-5}$	$1.6x10^{-6}$

In order to develop release fraction values for the sensitivity study accident categories, several parameters need to be defined. These parameters are defined in Table D5-3.

Table D5-3 Definitions of Parameters used in the Sensitivity Study Accident Categories

F_{B1}	Fraction of fuel elements failed by the ships collision
F_{C1}	Release fraction for fission products from the fuel to the cask cavity due to the mechanical effects of the ship collision
F_{CE1}	Fraction of the fission products released to the cask cavity that escape from the cask in the absence of a fire
F_{FC2}	Fraction of fission products released from the fuel to cask cavity due to heating of the fuel from ambient temperature (T_a)to some elevated temperatures (T_f) less than 900°K
F_{B2}	Fraction of the fuel elements failed by burst rupture due to heating from T_a to T_f
F_{CE2}	1 - (T_a/T_f) where $T_a/T_f = V_a/V_f$ = the fraction of the gases in the cask at ambient temperature that remain in the cask after heating to Tf
F_{FC3}	Fraction of fission products released from the fuel to the cask cavity after the fuel has been heated to T_{FC3}(=temperature where aluminum-uranium fuel melts and TRIGA fuel burns if exposed to air
F_{B3}	The fraction of fuel elements failed by burst rupture due to heating from T_{FC3} to T_f
F_{CE3}	1 - (T_{FC3}/T_f) where $T_{FC3}/T_f = V_{TC3}/V_f$ = the fraction of the gases in the cask after heating to T_{FC3} that remain in the cask after further heating to T_f

Then, the release fraction (F_{R4}) for Category 4 events is given by

$$F_{R4} = F_{B1}F_{FC1}F_{CE1} \quad (1)$$

If the collision leads to a fire that heats the cask to elevated temperatures that do not exceed 900°K (1160°F) heating of the fuel may cause more fission products to be released from the fuel to the 900° cask cavity, and expansion of cask gases due to heating by the fire will cause a substantial fraction of the gas borne fission products to be transported from the cask interior through the failed cask seal to the environment. Thus, the release fraction (F_{R5A}) for Category 5A events is given by

$$F_{R5A} = F_{R4} + F_{B1}F_{FC1}(1 - F_{CE1})F_{CE2} + F_{B2}F_{FC2}F_{CE2} \quad (2)$$

If the collision has led to cask failures (a single medium hole or two smaller holes) that allow substantial convective flow through the cask, then all fission products released to the cask interior will be transported from the cask to the environment. Thus, the release fraction (F_{R6A}) for Category 6A events is given by

$$F_{R6A} = F_{R4} + F_{B1}F_{FC1}(1 - F_{CE1}) + F_{B2}F_{FC2} \quad (3)$$

as by definition $F_{CE2} = 1.0$ for Category 6 events.

The release fraction (F_{R5B}) for fire events that heat the cask to temperatures above 900°K (1160°F), i.e. Category 5B events where Al-U alloy fuels melt and TRIGA fuel burns if exposed to oxygen is given by

$$F_{R5B} = F_{R5A} + F_{B3}F_{FC3}F_{CE3} \quad (4)$$

where

Again, if a Category 6 event has occurred, the release fraction (F_{R6B}) will be

$$F_{R6B} = F_{R6A} + F_{B3}F_{FC3} \quad (5)$$

since by definition $F_{CE3} = 1.0$ for Category 6 events.

The release fractions used in the base case assessment are the same as those (Wilmot 1981) developed for air-cooled casks for release of fission products from spent commercial UO_2 fuel for three processes: impact, burst, and oxidation. Base case Category 4 release fractions are the same as those developed by Wilmot for impact events involving air-cooled casks. Except for cesium, Category 5 release fractions are equal to the sum of Wilmot's release fractions for impact and burst, and Category 6 release fractions are equal to the sum of Wilmot's release fractions for impact, burst, and oxidation. For cesium, the base case uses release fractions that have been adjusted somewhat to reflect the effect of metallic fuel properties on cesium release. This information is used as the basis to derive several of the values for the parameters identified in Table D5-3.

For impact events, Wilmot uses $F_{B1} = 0.1$, $F_{FC1} = 0.2$ and $F_{CE1} = 0.5$ for krypton; and $F_{FC1} = 2x10^{-6}$ and $F_{CE1} = 0.05$ for cesium, ruthenium and particulates for release of fuel fines and thus the fission products trapped in the fines. For burst events, Wilmot assumes that $F_{B2} = 0.9$. Table D5-2 shows that the base case used values of 0.1, $9x10^{-4}$, $1x10^{-6}$, and $5x10^{-8}$, respectively, for the release fractions for krypton, cesuim, ruthenium, and particulates for Category 5 events. If Equation 2 is solved for F_{FC2} using the base case values for Category 5 events for F_{R5A} and Wilmot's values for F_{B1}, F_{B2}, F_{FC1}, and F_{CE1}, then the following values are obtained for F_{CE2}: 0.15 for krypton, $1.6x10^{-3}$ for cesium, $1.6x10^{-6}$ for ruthenium, and 0 for particulates.

The analysis presented in Attachment D4 of cask damage caused by impact and crush concludes that damage will not result from the impacts forces experienced by cask during ship collisions, and that if the cask is subjected to crush forces, they will always be large enough to fail all of the fuel elements contained in the cask. Therefore, $F_{B1} = F_{B2} = F_{B3} = 1.0$.

To facilitate comparison of the new release fractions developed here to the release fractions used in the base case, the release fractions for the cesium, ruthenium, and particulate chemical element groups for Category 4 events were forced to be the same as the value used in the base case. Although aluminum-uranium alloy fuels should have very little, if any, fuel fines associated with the metal plates from which the fuel bundles are fabricated, to achieve this equivalence, it was assumed that aluminum-uranium alloy fuels have amounts of fuel fines one-tenth of those assumed by Wilmot for uranium dioxide fuels. Thus, for aluminum-uranium alloy fuels, $F_{FC1} = 2x10^{-7}$ and therefore, because $F_{B1} = 1.0$, $F_{R4} = 2x10^{-8}$, which is the value that the base case used for the realease fraction for cesium, ruthenium, and particulate for Category 4 events.

Reasonable choices for F_{FC3} for aluminum-uranium alloy fuels, that is, for release to the cask cavity upon melting for the alloy fuel, are 1.0 for krypton, 0.1 for cesium, $1.6x10^{-5}$ for ruthenium, and $1.6x10^{-6}$ for particulate, where ruthenium release from metallic fuel upon melting has been assumed to be ten times the ruthenium release from commercial uranium dioxide fuel estimated for Category 5A events (the value of F_{FC2} for ruthenium release from uranium dioxide fuel for Category 5A events. Particulate release has been assumed to be about the same as ruthenium release from uranium dioxide fuel for Category 5A events and about ten times larger than particulate releases from aluminum-uranium alloy fuels for Category 4 events (the value of F_{FC1} for particulate release from aluminum-uranium alloy fuels for Category 4 events), as the melting of aluminum uranium alloy fuels due to heating of the cask by a fire is not likely to be violent.

Reasonable choices for F_{FC3} for TRIGA fuel are 1.0 for krypton; 0.3 for cesium; 0.3 for ruthenium, since burning of the fuel means that ruthenium will be converted to a volatile oxide by exposure to air; and 0.01 for particulate, on the assumption that the high exothermicity of the combusion process will cause one percent of the fuel mass to be aerosolized. For Category 5B, these values were decreased by a factor of 3, because air can only enter the cask due to cooling, which will not lead to fuel burning if the fuel cools

below 900°K, (1160°F). Even if burning does occur, efficient transport of fission products released by the burning from the cask to the environment can occur only by gas expansion caused by the heat released by fuel burning. Thus, the cask atmosphere must breath (pass through several cooling/burning cycles), if significant quantities of fission products are to be released by fuel burning, when there is no convective flow of air through the cask.

Table D5-4 lists the parameters used in Equations 1 through 5, and presents the values used for each parameter to calculate values for the release fractions F_{R4}, F_{R5A}, F_{R6A}, F_{R5B}, and F_{R6B}. For the four EA5 results for UO_2 fuel, the result calculated is the F_{FC2} value, not the F_{R5} value, which is an input and is set equal to the value used in the EA for the indicated element group.

Table D5-4 Parameters Used to Generate High Temperatures Fire Sensitivity Study Release Fractions

Accident Category	*Fuel*	*Element*	*Parameter*[1]									
			F_{B1}	F_{C1}	F_{CE1}	F_{B2}	F_{FC2}	T_a	T_{FC3}	T_f	F_{FC3}	F_R
Base Case 4		krypton	0.1	0.2	0.5							0.01
		all others	0.1	$2x10^{-6}$	0.05							$1x10^{-8}$
Base Case 5		krypton	0.1	0.2	0.5	0.9	0.15	300		800		0.1
		cesium	0.1	$2x10^{-6}$	0.05	0.9	$1.6x10^{-3}$	300		800		$9x10^{-4}$
		ruthenium	0.1	$2x10^{-6}$	0.05	0.9	$1.6x10^{-6}$	300		800		$1x10^{-6}$
		particulates	0.1	$2x10^{-6}$	0.05	0.9	0.0	300		800		$5x10^{-8}$
Sensitivity Study 4	Al-U	all	1.0	$2x10^{-7}$	0.05							$1x10^{-8}$
	TRIGA	krypton	1.0	0.2	0.5							0.1
	TRIGA	all others	1.0	$2x10^{-6}$	0.05							$1x10^{-7}$
Sensitivity Study 5A	TRIGA	krypton	1.0	0.2	0.05	1.0	0.15	300		800		0.26
	TRIGA	cesium	1.0	$2x10^{-6}$	0.05	1.0	$1.6x10^{-3}$	300		800		0.001
	TRIGA	ruthenium	1.0	$2x10^{-6}$	0.05	1.0	$1.6x10^{-6}$	300		800		$2.3x10^{-6}$
	TRIGA	particulates	1.0	$2x10^{-6}$	0.05	1.0	0.0	300		800		$1.3x10^{-6}$
	Al-U	all	1.0	$2x10^{-7}$	0.05	1.0	0.0	300		800		$1.3x10^{-7}$
Sensitivity Study 5B	TRIGA	krypton	1.0	0.2	0.5	1.0	0.15	300	923	1023	0.33	0.31
	TRIGA	cesium	1.0	$2x10^{-6}$	0.05	1.0	$1.6x10^{-3}$	300	923	1023	0.1	0.011
	TRIGA	ruthenium	1.0	$2x10^{-6}$	0.05	1.0	$1.6x10^{-6}$	300	923	1023	0.1	0.0098
	TRIGA	particulates	1.0	$2x10^{-6}$	0.05	1.0	0.0	300	923	1023	0.0033	$3.3x10^{-4}$
	Al-U	krypton	1.0	$2x10^{-7}$	0.05	1.0	0.0	300	923	1023	1.0	0.098
	Al-U	cesium	1.0	$2x10^{-7}$	0.05	1.0	0.0	300	923	1023	0.1	0.0098
	Al-U	ruthenium	1.0	$2x10^{-7}$	0.05	1.0	0.0	300	923	1023	$1.6x10^{-5}$	$1.7x10^{-6}$
	Al-U	particulates	1.0	$2x10^{-7}$	0.05	1.0	0.0	300	923	1023	1.6x10-6	$3.0x10^{-7}$
Sensitivity Study 6A	TRIGA	krypton	1.0	0.2	0.5	1.0	0.15	300		800		0.35
	TRIGA	cesium	1.0	$2x10^{-6}$	0.05	1.0	$1.6x10^{-3}$	300		800		0.0016
	TRIGA	ruthenium	1.0	$2x10^{-6}$	0.05	1.0	$1.6x10^{-6}$	300		800		$3.6x10^{-6}$
	TRIGA	particulates	1.0	$2x10^{-6}$	0.05	1.0	0.0	300		800		$2.0x10^{-6}$
	Al-U	all	1.0	$2x10^{-7}$	0.05	1.0	0.0	300		800		$2.0x10^{-7}$
Sensitivity Study 6B	TRIGA	krypton	1.0	0.2	0.5	1.0	0.15	300	923	1023	1.0	1.0
	TRIGA	cesium	1.0	$2x10^{-6}$	0.05	1.0	$1.6x10^{-3}$	300	923	1023	0.3	0.3
	TRIGA	ruthenium	1.0	$2x10^{-6}$	0.05	1.0	$1.6x10^{-6}$	300	923	1023	0.3	0.3
	TRIGA	particulates	1.0	$2x10^{-6}$	0.05	1.0	0.0	300	923	1023	0.01	0.01
	Al-U	krypton	1.0	$2x10^{-7}$	0.05	1.0	0.0	300	923	1023	1.0	1.0
	Al-U	cesium	1.0	$2x10^{-7}$	0.05	1.0	0.0	300	923	1023	0.1	0.1
	Al-U	ruthenium	1.0	$2x10^{-7}$	0.05	1.0	0.0	300	923	1023	$1.6x10^{-5}$	$1.6x10^{-5}$
	Al-U	particulates	1.0	$2x10^{-7}$	0.05	1.0	0.0	300	923	1023	$1.6x10^{-6}$	$1.8x10^{-6}$

Inspection of Table D5-2 allows the size of the new release fractions developed for aluminum-uranium alloy and TRIGa fuels to be conpared to the release fractions used in the base case calculations. Table D5-5 summarizes these comparisons.

Table D5-5 Relative Size of the Sensitivity Study Release Fractions Compared to the Base Case Release Fractions Used to Perform the Base Case Calculations

Fuel	*Severity Category*		*Size of New Sensitivity Study Release Fractions Compared to Base Case Release Fractions*
	Sensitivity Study	*Base Case*	
Aluminum-Uranium Alloy	4	4	About the same (krypton much smaller)
	5A	5	Smaller (cesium 10,000 times smaller)
	5B	5	Cesium 10 times larger
	6A	6	Cesium 5000 times smaller
	6B	6	Cesium 100 times larger
TRIGA	4	4	10 times larger
	5A	5	About the same
	5B	5	Cesium 10 times larger
	6A	6	About the same
	6B	6	Cesium 300 times larger

D5.4 Probability of High-Temperature Events

Data on the temperatures of real ship fires is nearly non-existent. Only one of the five severe fires identified by searching the Lloyd's of London data (Lloyd's, 1991) attained temperatures where steel beams buckled due to thermal stress. Carbon steels begin to soften at about 475°K (395°F) and have lost 90 percent of their strength at about 925°K (1,205°F). Thus, buckling of ship structures due to thermal stress might be expected to occur at about 700°K (800°F), the midpoint of this temperature range, which suggests that one severe fire in five attains temperatures at about 700°K (800°F) and also that P_{T900K} is less than 0.2. Due to the lack of ship board fire temperature data the an attempt has been made to estimate the likelihood of a fire that exceeds 900°K (1160°F).

A shipboard fire can heat the contents of a transportation cask to temperatures above 900°K (1,160°F) only if three conditions are met: (1) the fire must consume a high quality fuel such as gasoline or jet fuel, (2) enough fuel must be available to cause the fire to burn for an hour or more, and (3) the fire cannot be smothered by lack of air or the operation of fire suppression systems. Most severe ships fires involve the burning of the ship's own fuel (bunker or diesel fuel) or of crude oil, when the collision that leads to the fire involves an oil tanker. Thus, P_{T900K}, the chance that a ship fire can heat the contents of a transportation cask to temperatures above 900°K (1,160°F), can be estimated as follows:

$$PT>900K = P_{good\ fuel} \times P_{enough\ fuel} \times P_{enough\ oxygen}$$

Diesel fuel, bunker fuel, and crude oil all have peak flame temperatures that exceed 900°K or 1,160°F (Mudan, 1988), and most polymeric materials (e.g., plastics, wood) have peak flame temperatures of about 1,200°K or 1,700°F (Babrauskas, 1986a). Since fires in cargo holds should behave like enclosure fires, hold fires that burn wood could attain peak temperatures of about 1200°K (1,700°F), if post flashover conditions are attained (Babrauskas, 1986a). So, the fuels and solid materials that are likely to be involved in shipboard fires in cargo holds should be able to heat cask contents to temperatures significantly above

900°K (1,160°F), provided the fire burns long enough and isn't suppressed by lack of oxygen or the operation of fire suppression systems. Thus, $P_{good\ fuel}$, the chance that a long burning hold fire is supported by the burning of a good fuel, is not likely to be small and is here assumed to be 0.9.

The review of ship fires prepared by the French Bureau Veritas for the International Maritime Organization (IMO, 1992) contains data on ship fire durations. Most ship fires (70 to 80 percent) do not burn for an hour. However, most severe ship fires (95 percent) burn for more than an hour. Therefore, the chance that a severe fire involves enough fuel to burn for an hour or more, $P_{enough\ fuel}$, is assumed to be 0.95.

Figure D5-1 presents an event tree for oxygen availability during fires in cargo holds, and is used to estimate $P_{enough\ oxygen}$. The tree shows that most cargo hold fires will be partially starved for oxygen for two reasons, because hold covers will be closed when the fire starts, or will be deliberately closed after it starts in order to smother the fire; or because CO_2 fire suppression systems are installed in the hold and operate successfully. To quantify the event tree provided in Figure D5-1, it was necessary to derive the probability of these two events. The probability that a cargo hold is closed during a collision can be estimated using the following relationship.

$$P_{closed} = 1 - P_{open}$$

where

$$P_{open} = P_{all\ not\ closed} P_{worked} P_{location} \sum (N_i P_{deck}).$$

The derivation of each of the terms in this relationship is described in the following paragraphs.

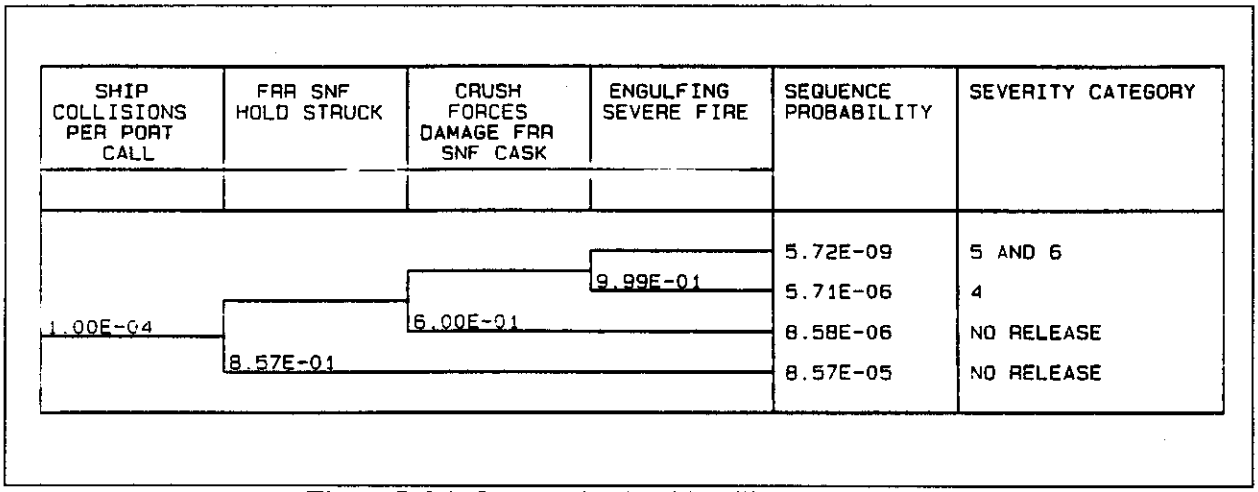

Figure D5-1 Oxygen Availability Given a Hold Fire

Cargo hold covers are normally closed except during loading of unloading of cargo. Thus, if a typical port call takes approximately three days (half a day entering the port and docking, two days anchored at the dock with two-thirds of that time, (two eight-hour shifts per day) spent loading and unloading cargo, and one-half day leaving the port) then all holds will be closed about half of the time while a ship is in port. Conversely, about half of the time at least one hold will be open. Thus $P_{all\ not\ closed} = \frac{1}{2}$ or 0.5.

When a break-bulk freighter like the seven-hold ship used in these analyses is being loaded or unloaded, usually three or four holds are being worked at any given time. Thus, when the ship is being loaded or unloaded, P_{worked}, the probability that a given hold is being worked is ½ or 0.5.

The break-bulk freighter used in these analyses has seven holds. Five of these holds contain three cargo decks, one contains four cargo decks, and one contains only two cargo decks. Thus, there are 21 possible deck locations for a spent fuel cask in this typical ship. Accordingly, $P_{location}$, the chance that a spent nuclear fuel cask has been loaded onto a given deck in one of the seven holds is 0.048.

All hold openings have covers, not just the opening in the main deck through which the hold is loaded and unloaded, but also the openings in the cargo decks within each hold. When a deck in a cargo hold is being loaded or unloaded, all openings above that deck must be open and the opening in the deck and all openings in lower decks are normally closed. Thus, while a hold is being worked, upper decks in that hold will be open to outside air more often than lower decks. For example, for a three-deck hold, while the hold is being worked, the upper deck will always be open to the outside air, the second deck will be open about two-thirds of the time, and the lowest deck will be open about one-third of the time. Thus, if N is the number of holds with two, three, or four decks, and P_{deck} is the probability that deck i in a hold is open to outside air while that hold is being worked, then P_{closed}, the chance that an engulfing fire is partially starved for oxygen because there is a cargo deck or main deck hold cover in place between the fire and the outside air will be:

$$P_{closed} = 1 - \{(0.5)(0.5)(0.048)([5(1 + \tfrac{2}{3} + \tfrac{1}{3})] + [1(1 + \tfrac{3}{4} + \tfrac{1}{2} + \tfrac{1}{4})] + [1(1 + \tfrac{1}{2})])\}$$

$$= 0.833$$

The ORI study (ORI, 1981a) found that over half (60 percent) of all cargo ships are equipped with fire detectors and CO_2 fire suppression systems. Because CO_2 fire suppression systems are not complicated, they should operate reliably on demand most of the time. To be conservative, failed operation during one of five fire events is assumed.

Using this data, the event tree in Figure D5-1 can be quantified to determine the probability of the event $P_{enough\ oxygen}$. Two branches of the oxygen availability tree lead to the outcome "enough air." The probabilities of these two branches sum to 0.087. Thus, 0.09 is a reasonable estimate for $P_{enough\ oxygen}$, the chance that a fire has adequate oxygen available to burn freely and generate maximum heat loads.

Combining the probability estimates for $P_{good\ fuel}$, $P_{enough\ fuel}$, and $P_{enough\ oxygen}$ allows $P_{T900\ K}$ to be estimated as follows:

$$P_{T900\ K} = P_{good\ fuel} \times P_{enough\ fuel} \times P_{enough\ oxygen}$$

$$= 0.9 \times 0.95 \times 0.09 = 0.077$$

Rounding to the next order of magnitude yields a conservative estimate of 0.1 for the chance that a severe engulfing fire with a duration of at least an hour will heat the contents of a transportation cask engulfed by the fire to temperatures significantly higher than 900°K (1,160°F).

D5.5 Probability of Convective Flow through the Failed Cask

Non-uniform heating of the cask during engulfing fires is expected to produce substantial flow of gases through the cask if two or more small holes or one medium hole have been produced in the cask by the ship collision. Because transportation casks bottoms and lid seats are welded to the cylindrical shell of the cask using full-penetration welds that are as strong or stronger than the parent material, when the cask shell is subjected to a severe stress (e.g, high impact or crush forces), the cask shell should yield before the welds fail. In fact, extra-regulatory 60 mph drop tests produced large plastic strains in the cylindrical shell of the test cask without failing its welds (Ludwigsen and Ammerman, 1995). Thus, during a ship collision, crush forces should collapse the cask walls inward without producing catastrophic failure of the lid, its seat, or the welds that attach the seat or the bottom of the cask to the cask walls. Therefore, an unusual configuration of cargo and/or deformed ship structures must be produced during the ship collision in order to subject the cask to forces that will produce failures substantially worse than failure of the lid seal. Either the lid seat must be bent significantly, or at least two penetrations must break, or the cask walls must be sheared or punctured. Although data for such failures is lacking, because casks normally do not fail by these mechanisms, the probability that a failure substantially worse than seal failure occurs is assumed to be no larger than 0.1.

D5.6 Severity Category Event Trees

Figures D5-2 and D5-3 present event trees that represent the sequence of events that lead to category 4, 5A, 5B, 6A, and 6B releases from transportation casks due to ship collisions. After rounding to the nearest integer, Figure D5-3 shows that these categories have the probabilities per port call provided in Table D5-4.

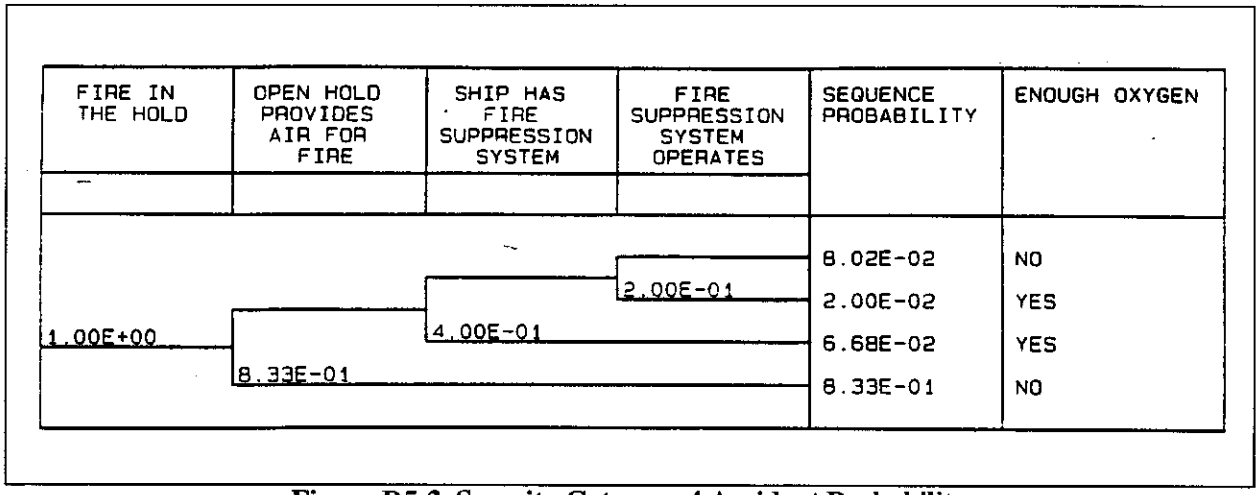

Figure D5-2 Severity Category 4 Accident Probability

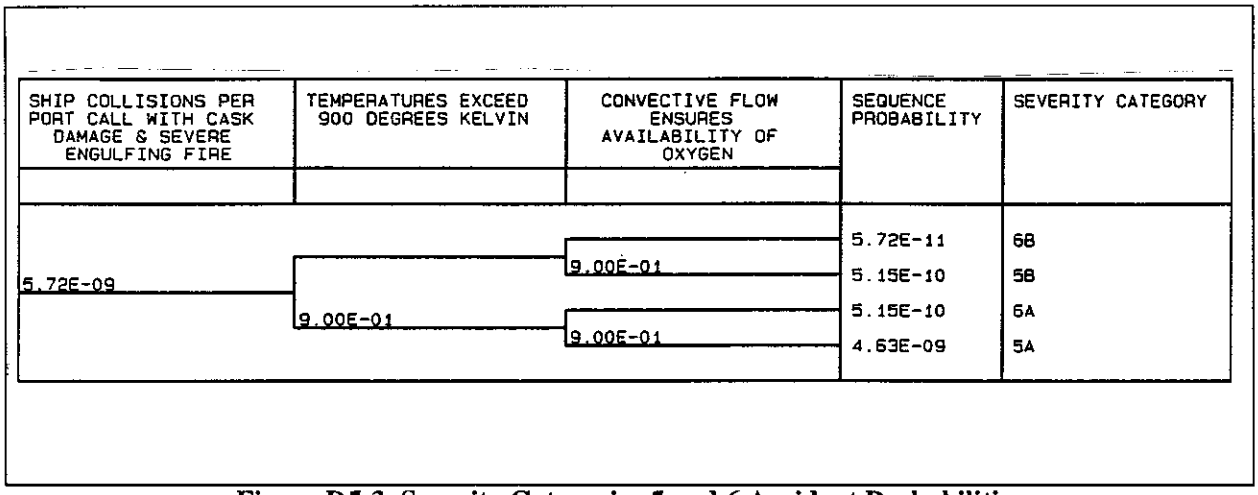

Figure D5-3 Severity Categories 5 and 6 Accident Probabilities

Table D5-4 Sensitivity Study Accident Severity Category Probabilities

Severity Category	*Probability Per Port Call*
4	$6x10^{-6}$
5A	$5x10^{-9}$
5B	$5x10^{-10}$
6A	$5x10^{-10}$
6B	$6x10^{-11}$